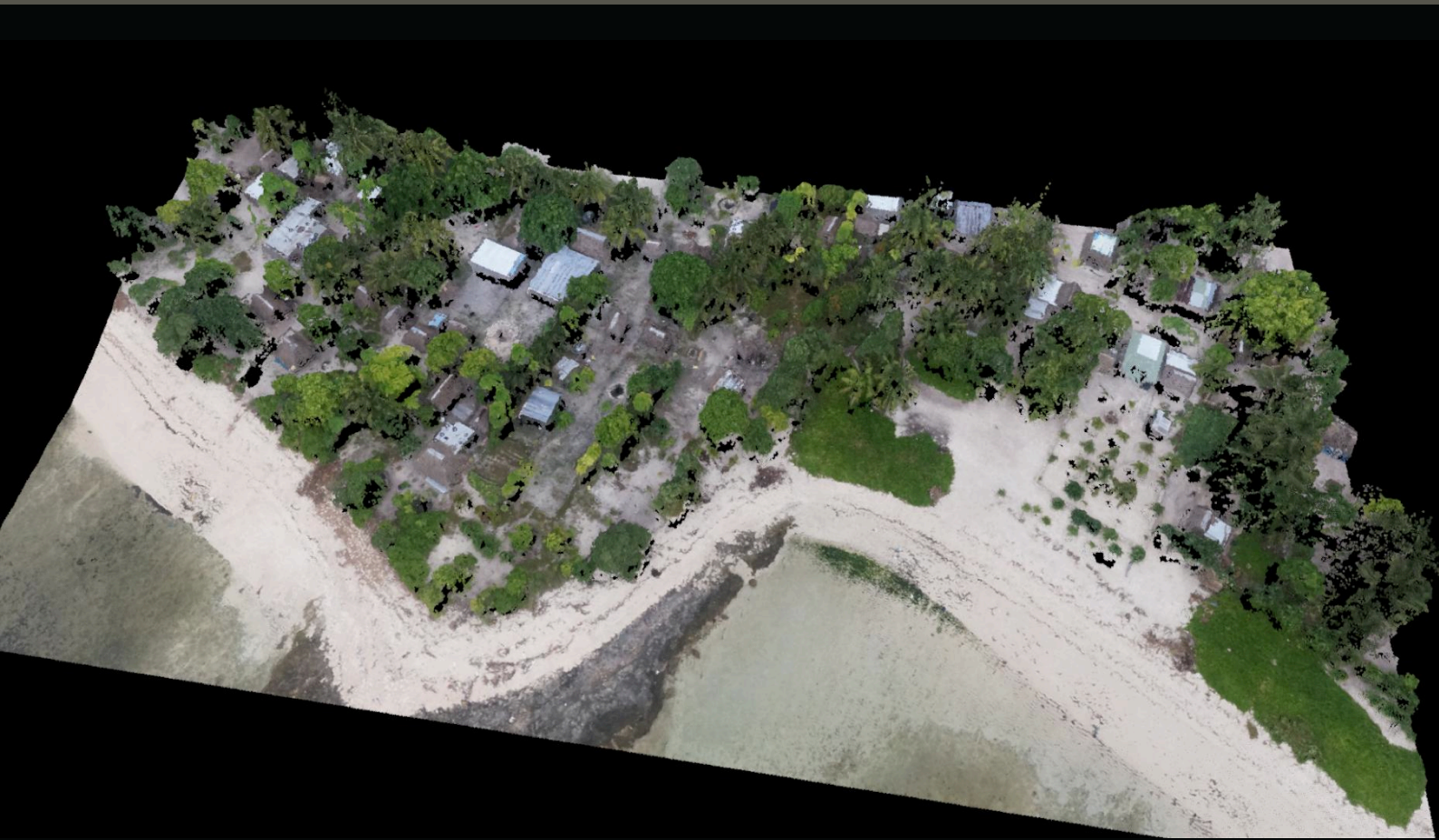


Bonriki Inundation Vulnerability Assessment

Land Use Mapping



Amrit Raj, Herve Damaliam, Jens Kruger



Australian Government



SPC
Secretariat
of the Pacific
Community



Australian
Aid 

Bonriki Inundation Vulnerability Assessment (BIVA)

Land Use Mapping

Amrit Raj

Herve Damlamian

Jens Kruger



©Copyright Secretariat of the Pacific Community (SPC) 2015

All rights for commercial / for profit reproduction or translation, in any form, reserved. SPC authorises the partial reproduction or translation of this material for scientific, educational or research purposes, provided that SPC and the source document are properly acknowledged. Permission to reproduce the document and/or translate in whole, in any form, whether for commercial / for profit or non-profit purposes, must be requested in writing. Original SPC artwork may not be altered or separately published without permission.

Original text: English

Secretariat of the Pacific Community Cataloguing-in-publication data

SPC Technical Report SPC00001

March 2015

SPC DISCLAIMER

While care has been taken in the collection, analysis, and compilation of the data, they are supplied on the condition that the Secretariat of Pacific Community shall not be liable for any loss or injury whatsoever arising from the use of the data.

Secretariat of the Pacific Community
Geoscience Division (GSD)
Private Mail Bag, GPO Suva, Fiji Islands
Telephone: (679) 338 1377
Fax: (679) 337 0040
Email: amrtr@spc.int
www.spc.int
www.sopac.org

This report has been produced with the financial assistance from the Secretariat of the Pacific Community.

Table of Contents

Acknowledgements	4
Glossary	5
List of Abbreviations	6
Executive Summary	1
1. Introduction	2
1.1. Background	2
1.2. Purpose of this report	3
1.3. Scope of this report	4
2. Methodology.....	4
2.1. Image processing	4
2.2. Supervised classification	6
2.3. Post-classification re-coding	6
2.4. Accuracy assessment	6
3. Results.....	8
4. Analysis	36
5. Conclusion.....	42
6. References	43

Tables

Table 1: Imagery used for land use classification	5
Table 2: Contingency error matrix for the aerial image, 1943	8
Table 3: Results of the accuracy assessment for the supervised classification: 1943 aerial image	9
Table 4: Error matrix (in pixels) of the accuracy assessment for the supervised classification: 1943 aerial image.....	9
Table 5: Kappa statistics of the accuracy assessment for the supervised classification: 1943 aerial image	9
Table 6: Contingency error matrix for the aerial image, 1968	11
Table 7: Results of the accuracy assessment for the supervised classification: 1968 aerial image	12
Table 8: Error matrix (in pixels) of the accuracy assessment for the supervised classification: 1968 aerial image	12
Table 9: Kappa statistics of the accuracy assessment for the supervised classification: 1968 aerial image	12
Table 10: Contingency error matrix for the aerial image, 1984	14
Table 11: Results of the accuracy assessment for the supervised classification: 1984 aerial image	15
Table 12: Error matrix (in pixels) of the accuracy assessment for the supervised classification: 1984 aerial image	15
Table 13: Kappa statistics of the accuracy assessment for the supervised classification: 1984 aerial image	15
Table 14: Contingency error matrix for the aerial image, 1998	18
Table 15: Results of the accuracy assessment for the supervised classification: 1998 aerial image	18
Table 16: Error matrix (in pixels) of the accuracy assessment for the supervised classification: 1998 aerial image	18
Table 17: Kappa statistics of the accuracy assessment for the supervised classification: 1998 aerial image	18
Table 18: Contingency error matrix for the IKONOS image, 2003	21
Table 19: Results of the accuracy assessment for the supervised classification: 2003 IKONOS image.....	21

Table 20: Error matrix (in pixels) of the accuracy assessment for the supervised classification: 2003 IKONOS image	21
Table 21: Kappa statistics of the accuracy assessment for the supervised classification: 2003 IKONOS image ..	22
Table 22: Contingency error matrix for the Quick Bird PS image, 2007	25
Table 23: Results of the accuracy assessment for the supervised classification: 2007 Quick Bird PS image	25
Table 24: Error matrix (in pixels) of the accuracy assessment for the supervised classification: 2007 Quick Bird PS image	25
Table 25: Kappa statistics of the accuracy assessment for the supervised classification: 2007 Quick Bird PS image	25
Table 26: Contingency error matrix (in pixels) for the Geo-Eye image, 2012.....	29
Table 27: Results of the accuracy assessment for the supervised classification: 2012 Geo-Eye image	29
Table 28: Error matrix (in pixels) of the accuracy assessment for the supervised classification: 2012 Geo-Eye image	29
Table 29: Kappa statistics of the accuracy assessment for the supervised classification: 2012 Geo-Eye image .	30
Table 30: Contingency error matrix for the UAV Ortho-photo, 2014.....	33
Table 31: Results of the accuracy assessment for the supervised classification: 2014 UAV Ortho-photo.....	33
Table 32: Error matrix (in pixels) of the accuracy assessment for the supervised classification: 2014 UAV Ortho-photo	33
Table 33: Kappa statistics of the accuracy assessment for the supervised classification: 2014 UAV Ortho-photo	34
Table 34: Area calculation of classified categories for images	36

Figures

Figure 1. Bonriki Water Reserve Location	3
Figure 2. Bonriki Inundation Vulnerability Assessment project components	4
Figure 3: User-defined points used for accuracy assessment	7
Figure 4: Geo-referenced aerial image, 1943 – used for land use classification	8
Figure 5: Land use classification for aerial image, 1943	10
Figure 6: Geo-referenced aerial image, 1968 – used for land use classification	11
Figure 7: Land use classification for aerial image, 1968	13
Figure 8: Geo-referenced aerial image, 1984 – used for land use classification	14
Figure 9: Land use classification for aerial image, 1984	16
Figure 10: Geo-referenced image, 1998 – used for land use classification	17
Figure 11: Signature Mean Plot for classifications in aerial image, 1998	17
Figure 12: Land use classification for aerial image, 1998	19
Figure 13: IKONOS image (false colour composite), 2003 – used for land use classification	20
Figure 14: Signature Mean Plot for classifications in the IKONOS image, 2003	20
Figure 15: Land use classification for the IKONOS image, 2003	23
Figure 16: Quick Bird PS image, 2007 – used for land use classification	24
Figure 17: Signature Mean Plot for classifications in Quick Bird PS, 2007	24
Figure 18: Land use classification for Quick Bird PS image, 2007.....	27
Figure 19: Geo-Eye image (false colour composite), 2012 – used for land use classification	28
Figure 20: Signature Mean Plot for classifications used in Geo-Eye, 2012.....	28
Figure 21: Land use classification for Geo-Eye image, 2012.....	31
Figure 22: UAV Ortho-photo, 2014 – used for land use classification.....	32
Figure 23: Signature Mean Plot for classifications used in the UAV Ortho-photo	32
Figure 24: Land use classification for UAV Ortho-photo, 2014	35

Figure 25: Vegetation area changes from 1968 to 2014	37
Figure 26: Grassland area changes from 1968 to 2014	38
Figure 27: Vegetation/grassland area changes from 1943 to 2014	38
Figure 28: Bareland (runway) area changes from 1943 to 2014	40
Figure 29: Buildings count changes from 1968 to 2014	41
Figure 30: Monthly Tarawa rainfall – annual mean, 1950 to 2014	41

Acknowledgements

The BIVA project is part of the Australian Government's Pacific-Australia Climate Change Science and Adaptation Planning Program (PACCSAP), within the International Climate Change Adaptation Initiative. The project was developed by the Secretariat of the Pacific Community's (SPC) Geoscience Division (GSD) in partnership with the Australian Government and the Government of Kiribati (GoK).

This report was made possible through the contributions of a large number of people, who assisted during field surveys and data processing.

Key GoK stakeholders that contributed to the implementation of the project were:

- Ministry of Environment, Lands and Agricultural Development
- Ministry of Fisheries and Marine Resources Development
- Ministry of Civil Aviation
- Ministry of Public Works and Utilities (MPWU), in particular the Water Engineering Unit with the MPWU
- The Public Utilities Board (PUB), in particular the Water and Sanitation Division and the Customer Relations Division within the PUB
- The Office of the President, in particular the Disaster Management Office
- Members of the Kiribati National Expert Group on climate change and disaster risk management (KNEG)

The Bonriki Village community members also played a key role in the implementation of the project. Community members participated in the school water science and mapping program, assisted with construction of new piezometers and data collection for the groundwater component, and shared their knowledge and experiences with regards to historical inundation events and coastal processes.

Key technical advisors involved with implementation of the project included:

- Flinders University, Adelaide, Australia
- University of Western Australia, Perth, Australia
- The University of Auckland, Auckland, New Zealand
- United Nations Educational, Scientific and Cultural Organization, Institute for Water Education (UNESCO-IHE), Delft, the Netherlands
- Technical advisors Tony Falkland and Ian White

Glossary

- Maximum likelihood:** This refers to a decision rule that is based on the probability that a pixel in an image belongs to a particular classification. The basic equation assumes that these probabilities are equal for all classifications, and that the input bands have normal distributions.
- Contingency matrix:** Evaluate signatures that have been created from areas of interest (AOIs) in the image.
- Kappa value or coefficient:** A number that expresses the proportionate reduction in error generated by a classification process compared with the error of a completely random classification.

List of Abbreviations

BIVA	Bonriki Inundation Vulnerability Assessment
CCA	Ministry of Civil Aviation, Kiribati
GW	Ground water
GoK	Government of Kiribati
KNEG	Kiribati National Expert Group
LULC	Land use/land cover
ML	Maximum likelihood classification algorithm
PACCSAP	Pacific-Australia Climate Change Science and Adaptation Planning Program (Australian Government)
PUB	Public Utilities Board
SPC	Secretariat of the Pacific Community

Executive Summary

Land use/land cover is regarded as an important link to better understanding the interactions of human activities with the environment. In order to gain a full picture of these interactions it is necessary to monitor and detect land use/land cover changes over time. Remote sensing techniques are used to monitor land use changes such as urban and rural development and the use of natural resources.

The Bonriki Inundation Vulnerability Assessment (BIVA) project aims to assess the probability of salt water intrusion into the freshwater lens. The quality of the freshwater lens is highly correlated with the activities occurring on the land above it. In order to better understand the stress put upon the water reserve in the subject area over time, historical aerial photographs and high resolution satellite images were used to derive land use/land cover (LULC) for Bonriki. In this study, the following historical visual data were used:

- Aerial photographs from 1943, 1968, 1984 and 1998.
- Satellite images from 2003, 2007 and 2012.
- A 2014 Orthophoto derived from a Trimble unmanned aircraft system (UAS) survey.

The LULC baseline was computed using a supervised classification.

The land use in the subject area was described with the following classifications: bareland, vegetation, grassland and saltwater marsh. The assessment revealed a significant change in the land use categories in the subject area during the period 1943 to 1968. In 1943, 48.29% of the area was bareland, which had decreased to 17.78% by 1968. The study showed a significant change in vegetation and grassland (combined), from 46.81% in 1943, to 77.45% in 1968. By 1984 the area of land that was vegetation and grassland had decreased by 10.74%, to 66.70% of land area. From 1998 to 2014 there were no significant changes in bareland or vegetation/grassland (changes ranged between 1% and 5% over that period). The study revealed no significant change in the percentage of saltwater marsh classification between 1943 and 2014.

1. Introduction

1.1. Background

The Bonriki Inundation Vulnerability Assessment (BIVA) project is part of the Australian government's Pacific–Australia Climate Change Science and Adaptation Planning Program (PACCSAP), within the International Climate Change Adaptation Initiative. The objectives of PACCSAP are to:

- improve scientific understanding of climate change in the Pacific;
- increase awareness of climate science, impacts and adaptation options; and
- improve adaptation planning to build resilience to climate change impacts.

The BIVA project was developed by the Geoscience Division (GSD) of the Secretariat of the Pacific Community (SPC) in partnership with the Australian government and the Government of Kiribati (GoK).

1.1.1. *Project objective and outcomes*

The BIVA project aims to improve our understanding of the vulnerability of the Bonriki freshwater reserve to coastal hazards and climate variability and change. Improving our knowledge of risks to this freshwater resource will enable better adaptation planning by the GoK.

More specifically, the project has sought to use this knowledge to support adaptation planning through the following outcomes:

- Improved understanding and ability to model the role of reef systems in the dissipation of ocean surface waves and the generation of longer-period motions that contribute to coastal hazards.
- Improved understanding of freshwater lens systems in atoll environments with respect to seawater overtopping and infiltration, as well as current and future abstraction demands, recharge scenarios and land-use activities.
- Enhanced data to inform a risk-based approach in the design, construction and protection of the Bonriki water reserve.
- Increased knowledge provided to the GoK and the community of the risks associated with the impact of coastal hazards on freshwater resources in response to climate change, variability and sea-level rise.

1.1.2. *Context*

The Republic of Kiribati is located in the Central Pacific and comprises 33 atolls in three principal island groups. The islands are scattered within an area of about 5 million square kilometres. The BIVA project focuses on the Kiribati National Water Reserve of Bonriki. Bonriki is located on Tarawa atoll within the Gilbert group of islands in Western Kiribati (**Error! Reference source not found.**). South Tarawa is the main urban area in Kiribati, with the 2010 census recording 50,182 people of the more than 103,058 total population (KNSO and SPC 2012). Impacts to the Bonriki water resource from climate change, inundation, abstraction and other anthropogenic influences have potential for severe impacts on people's livelihood of South Tarawa. The Bonriki water reserve is used as the primary raw water supply for the Public Utilities Board (PUB) reticulated water system. PUB water is the source of

potable water use by at least 67% of the more than 50,182 people of South Tarawa (KNSO and SPC 2012). Key infrastructure including the PUB Water Treatment Plant and Bonriki International Airport and residential houses are also located on Bonriki, above the freshwater lens, making it an important economic, social and cultural area for the Republic of Kiribati.

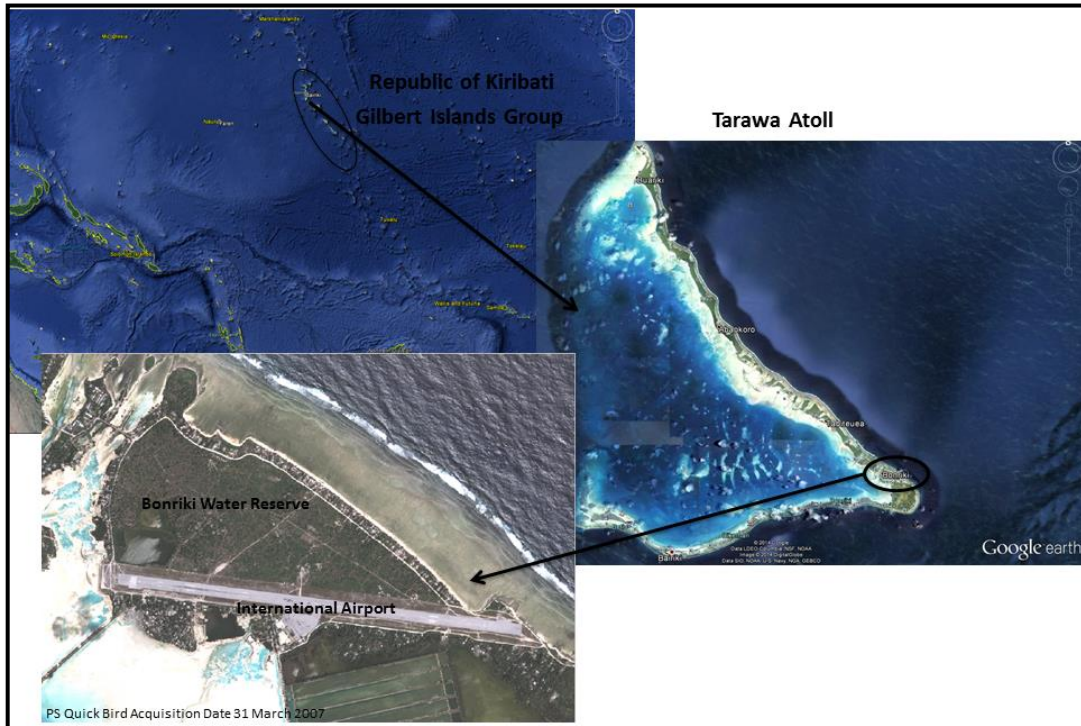


Figure 1. *Bonriki Water Reserve Location*

1.2. Purpose of this report

The purpose of this report is to provide a summary of the land use mapping activity undertaken as part of the BIVA project, and document outputs from this activity. As illustrated in Figure 2, the project consisted of three interlinked components: stakeholder engagement, groundwater investigations and analysis, and coastal investigations and analysis. Evidence of changes in land use, coastline and infrastructure were extracted through remote sensing techniques based on available high resolution satellite and aerial images. The land use mapping activity is part of the coastal component of the project and has primarily provided baseline data as input into the inundation model that was developed for the Bonriki area.

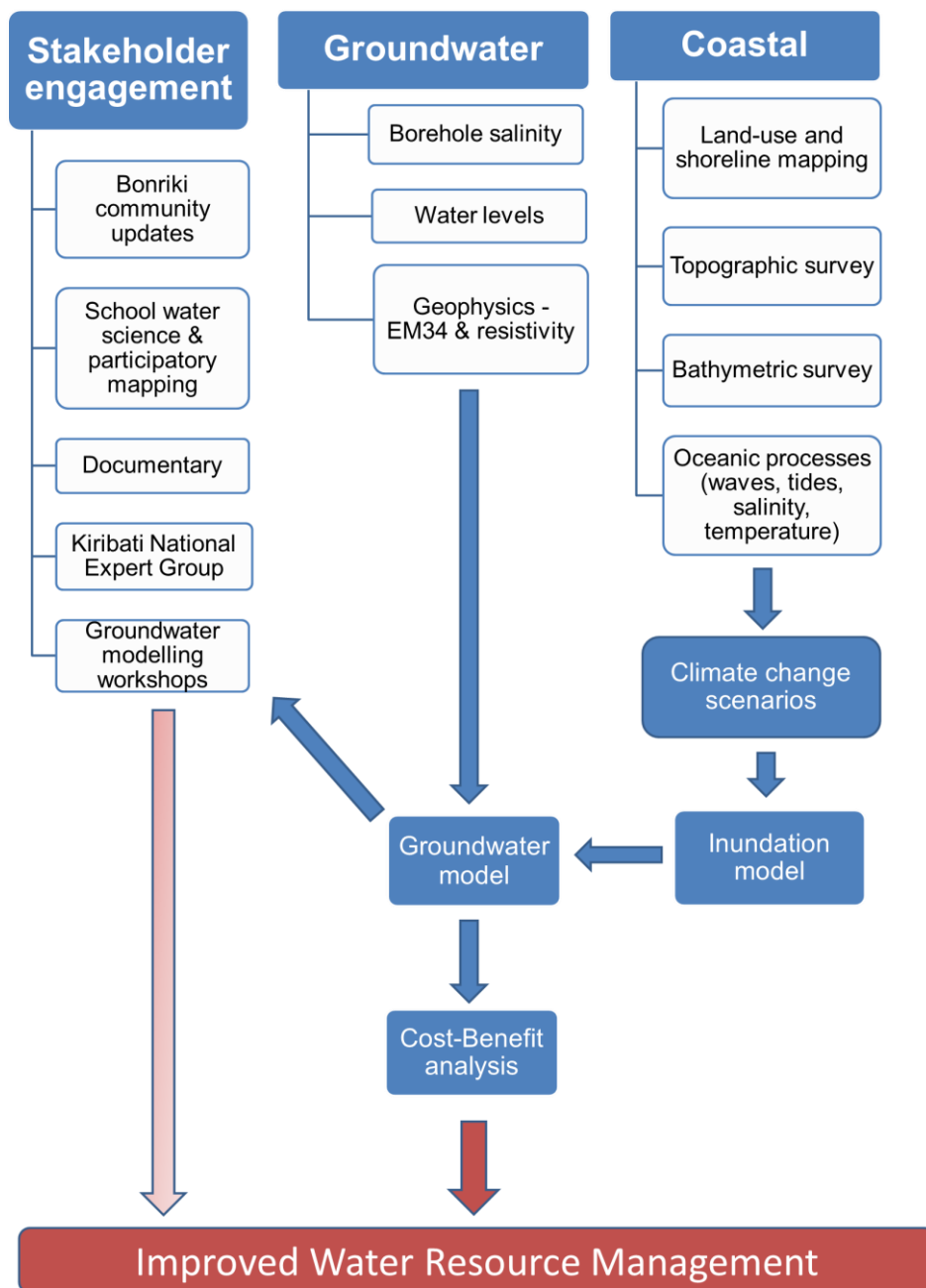


Figure 2. Bonriki Inundation Vulnerability Assessment project components

1.3. Scope of this report

This report describes changes in land use/land cover over a period of 71 years, using aerial and satellite imagery. The satellite images were processed using supervised classification techniques to produce land use maps, while infrastructure use was manually digitised. The land use map was used as a baseline to calculate changes over time.

2. Methodology

2.1. Image processing

The first step in the analysis was to compile available historical aerial photographs and satellite images of Bonriki, Kiribati. Historical aerial photographs were sourced for the years 1943, 1968, 1984 and 1998, and satellite images were obtained from the following satellites: IKONOS (2003), Quick Bird PS (2007) and Geo-Eye (2012). In August 2014, the team conducted a UAS survey (Topography Survey Report, SPC00003) over the site to expand the database with the latest possible imagery.

All aerial photographs were geo-rectified, which is the process of geo-referencing an image to a particular coordinate system, and then electronically manipulating these historical photographs so that they can be compared to current geo-referenced satellite images. The common projection used for the entire dataset is Universal Transverse Mercator Zone 59 North. The image manipulation and land use process was undertaken using ERDAS Imagine and GIS software ESRI Arc Map 10.

Table 1: Imagery used for land use classification

Image type	Year/month of acquisition	Resolution (meters)
Aerial photo	1943	1.0
Aerial photo	1968	0.30
Aerial photo	1984	0.60
Aerial photo	August 1998	0.25
IKONOS	December 2003	4.0
Quick Bird PS	March 2007	0.60
Geo-Eye	April 2012	0.50
UAV Ortho-photo	August 2014	0.10

Wherever visible, building footprints and roads were digitised. Low confidence is attributed to data extracted from the digitising of old black and white aerial photographs, as infrastructure, such as buildings and roads, is difficult to reliably detect on such images.

2.2. Supervised classification

Supervised classification is the process of using training samples – that is, samples of known identity – to classify pixels of unknown identity. Training samples are used to guide the classification algorithm in assigning specific spectral values to an appropriate information class. The training sample was selected by on-screen digitising.

The algorithm used for this classification was maximum likelihood. It is based on a statistical decision criterion to assist in the classification of overlapping signatures, where pixels are assigned to the class of highest probability. The maximum likelihood (ML) classification algorithm is the most common and appropriate classification method (Jonathan et al. 2007).

Supervised classification is applied by manually attributing several training samples to an identified information class. The number of classifications used per image depends on the number of spectral bands in the image. The number of classifications used in this study ranged from two, for black and white aerial imagery, to six, for multispectral (four-band) satellite imagery. Wherever possible, the image was clustered into the following six classifications: saltwater marsh, vegetation, grassland, buildings, bareland and runway. For the 2003 and 2012 images, cloud coverage obscures ground detail, so for these images cloud cover was added as a separate class. For the purposes of analysis, runway was combined with bareland. Only three classifications could be extracted from black and white imagery: vegetation, bareland and saltwater marsh.

2.3. Post-classification re-coding

Pixel-based supervised and unsupervised classification has limitations. For example, in false colour composite the reflectance calculated in shadow areas and water appears black. To overcome this problem the classified image need to be re-coded. Re-coding of misclassified categories was carried out using ERDAS Imagine software.

2.4. Accuracy assessment

After the re-coding of misclassified pixels, the accuracy assessment is carried out. This is a crucial step in assessing the reliability of the classified map. Without a proper accuracy assessment the image classification is considered incomplete. In order to determine the accuracy of the classification, a sample of pixels is selected on the classified image. The classification attributed to each pixel within the selected sample is compared with the ground reference data. In this case, a sample of 100 points homogeneously distributed across the study area has been selected, as shown in Figure 3. A classification error matrix (measured in pixels) is produced from this process, to quantify the quality of the classification.

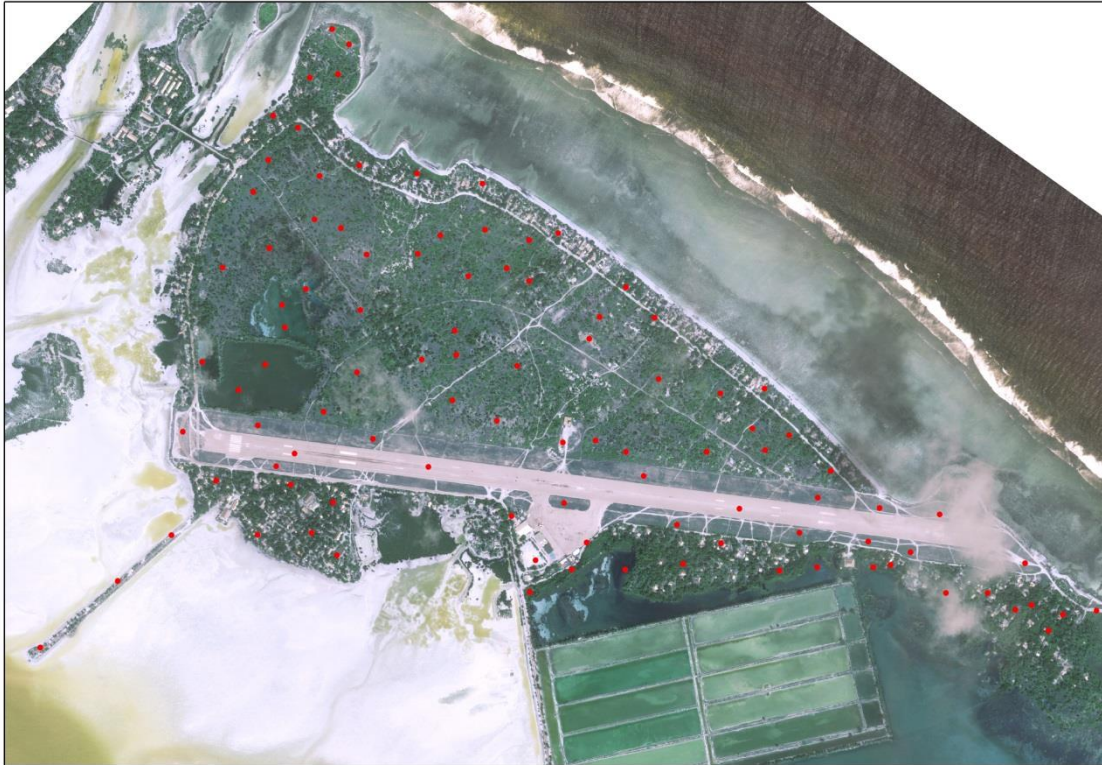


Figure 3: User-defined points used for accuracy assessment

The user's and producer's accuracy are widely used measurements for class accuracy. The producer's accuracy refers to the probability that a certain landcover of an area is classified correctly. The user's accuracy refers to the probability that a pixel classified as a certain landcover class in the map is in fact that class. The user's and producer's accuracy for any given class usually differ from one another.

Producer's accuracy is calculated by dividing the number of correctly classified pixels in each class by the number of training set pixels used for that class. User's accuracy is calculated by dividing the number of correctly classified pixels in each class by the total number of pixels that were classified in that class.

The outcome of the accuracy test is represented for each class by the kappa coefficient value (or K-value). Kappa analysis is a discrete multivariate technique, which calculates the overall accuracy for producers and users. A K-value of >0.8 represents a strong agreement, and therefore a good classification.

The last step in the classification process is to quantify over-time changes for each class, by undertaking area analysis, which calculates the percentage change in land use in a defined area. The 'count' field, which represents the number of cells in a particular raster category, is used to calculate the area in square metres (sq.m).

3. Results



Figure 4: Geo-referenced aerial image, 1943 – used for land use classification

Three training samples were assigned for the 1943 aerial photograph: vegetation, saltwater marsh and bareland. The image in Figure 4 indicates that Bonriki was used for multiple runways during the Second World War.

The image has only one band, which is not sufficient to differentiate between vegetation and grassland, so these were combined. Re-coding was carried out for saltwater marsh.

Table 2: Contingency error matrix for the aerial image, 1943

Classified data	Reference data (in pixels)			Row total
	Bareland	Saltwater	Vegetation	
Bareland	192227	0	0	192227
Saltwater	0	747	2188	2935
Vegetation	22	83	3725	3830
Column total	192249	830	5913	198992

Table 3: Results of the accuracy assessment for the supervised classification: 1943 aerial image

Classification	Reference total	Classified total	Number correct	Producer's accuracy	User's accuracy
Background	2	2	2	-----	-----
Saltwater marsh	7	7	7	100.00%	100.00%
Bareland	43	40	40	93.02%	100.00%
Vegetation	48	51	48	100.00%	94.12%
Total	100	100	97		
Overall classification accuracy = 96.00%					

Table 4: Error matrix (in pixels) of the accuracy assessment for the supervised classification: 1943 aerial image

Classification	Background	Saltwater marsh	Bareland	Vegetation	Total
Background	2	0	0	0	2
Saltwater marsh	0	7	0	0	7
Bareland	0	0	40	0	40
Vegetation	0	0	3	48	51
Total	2	7	43	48	100

Table 5: Kappa statistics of the accuracy assessment for the supervised classification: 1943 aerial image

Classification	Kappa
Background	1.0000
Saltwater marsh	1.0000
Bareland	1.0000
Vegetation	0.8869
Overall kappa value = 0.9309	

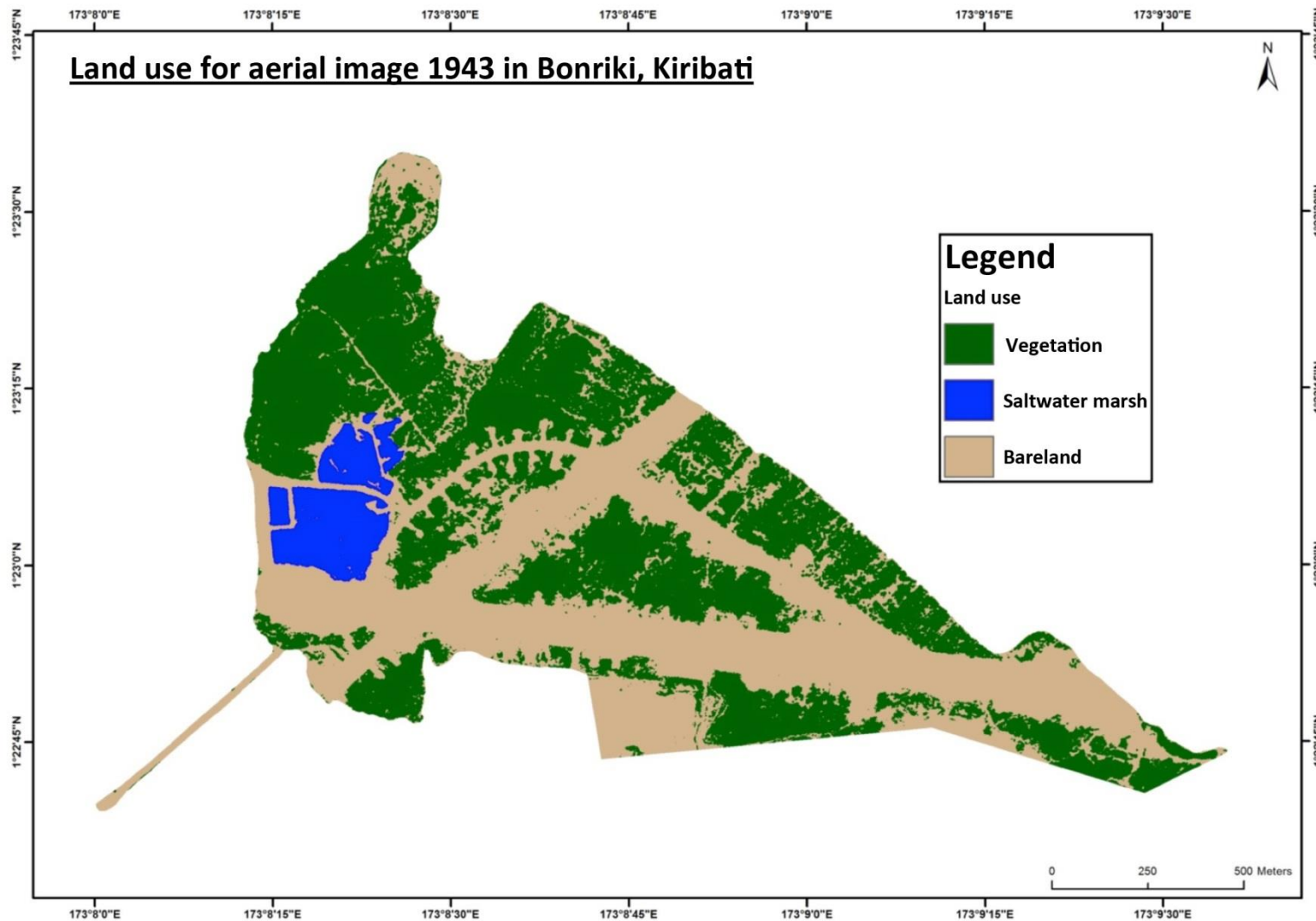


Figure 5: Land use classification for aerial image, 1943

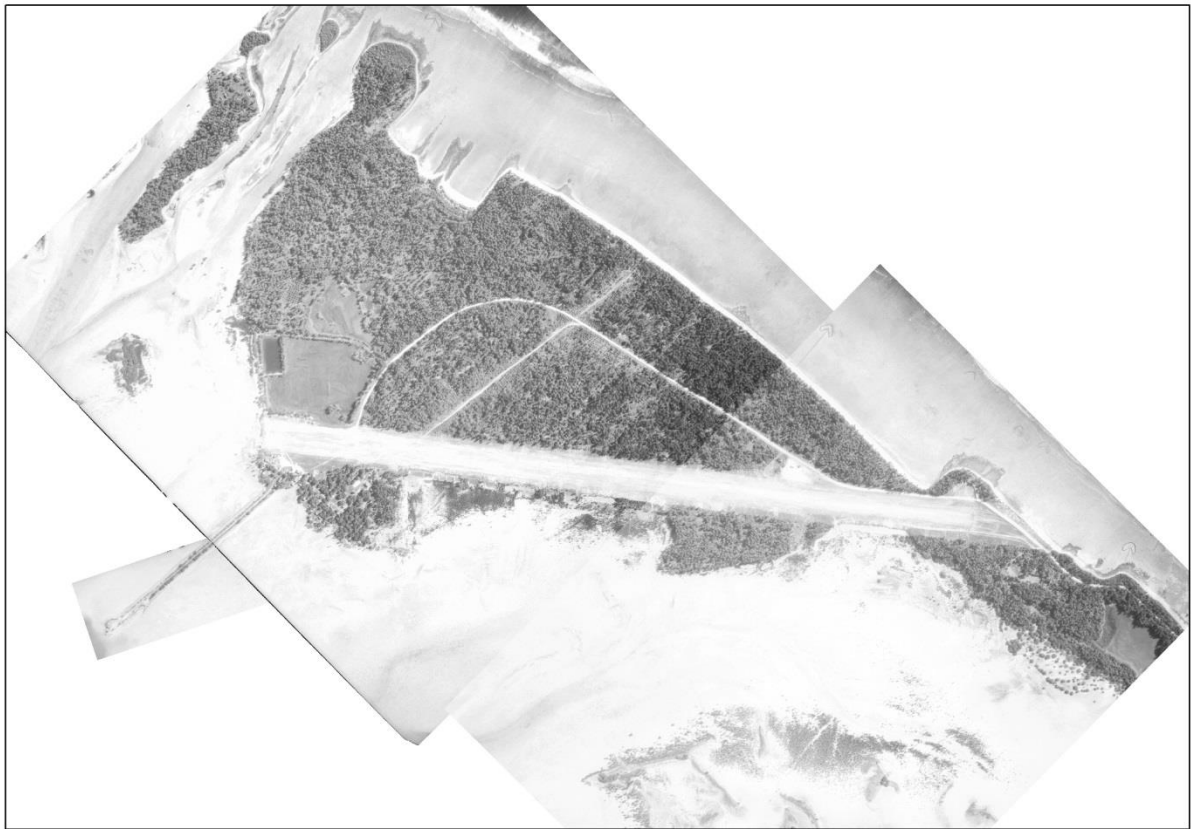


Figure 6: Geo-referenced aerial image, 1968 – used for land use classification

Four training samples were assigned for the 1968 aerial photograph: vegetation, grassland, saltwater marsh and bareland.

The image has only one band, which limits the number of classifications. Re-coding was carried out for saltwater marsh.

Table 6: Contingency error matrix for the aerial image, 1968

Classified data	Reference data (in pixels)			Row total
	Saltwater marsh	Vegetation	Bareland	
Saltwater marsh	806030	38562	15939	860531
Vegetation	71820	162583	0	234403
Bareland	2551	0	1393180	1395731
Column total	880401	201145	1409119	2490665

Table 7: Results of the accuracy assessment for the supervised classification: 1968 aerial image

Classification	Reference total	Classified total	Number correct	Producer's accuracy	User's accuracy
Background	10	10	10	-----	-----
Grassland	8	24	7	87.50%	29.17%
Bareland	21	21	21	100.00%	100.00%
Vegetation	61	45	44	72.13%	97.78%
Total	100	100	82		
Overall classification accuracy = 82.00%					

Table 8: Error matrix (in pixels) of the accuracy assessment for the supervised classification: 1968 aerial image

Classification	Background	Grassland	Bareland	Vegetation	Total
Background	10	0	0	0	10
Grassland	0	7	0	17	24
Bareland	0	0	21	0	21
Vegetation	0	1	0	44	45
Total	10	8	21	61	100

Table 9: Kappa statistics of the accuracy assessment for the supervised classification: 1968 aerial image

Classification	Kappa
Unclassified	1.0000
Grassland	0.2301
Bareland	1.0000
Vegetation	0.9430
Overall kappa value = 0.7240	

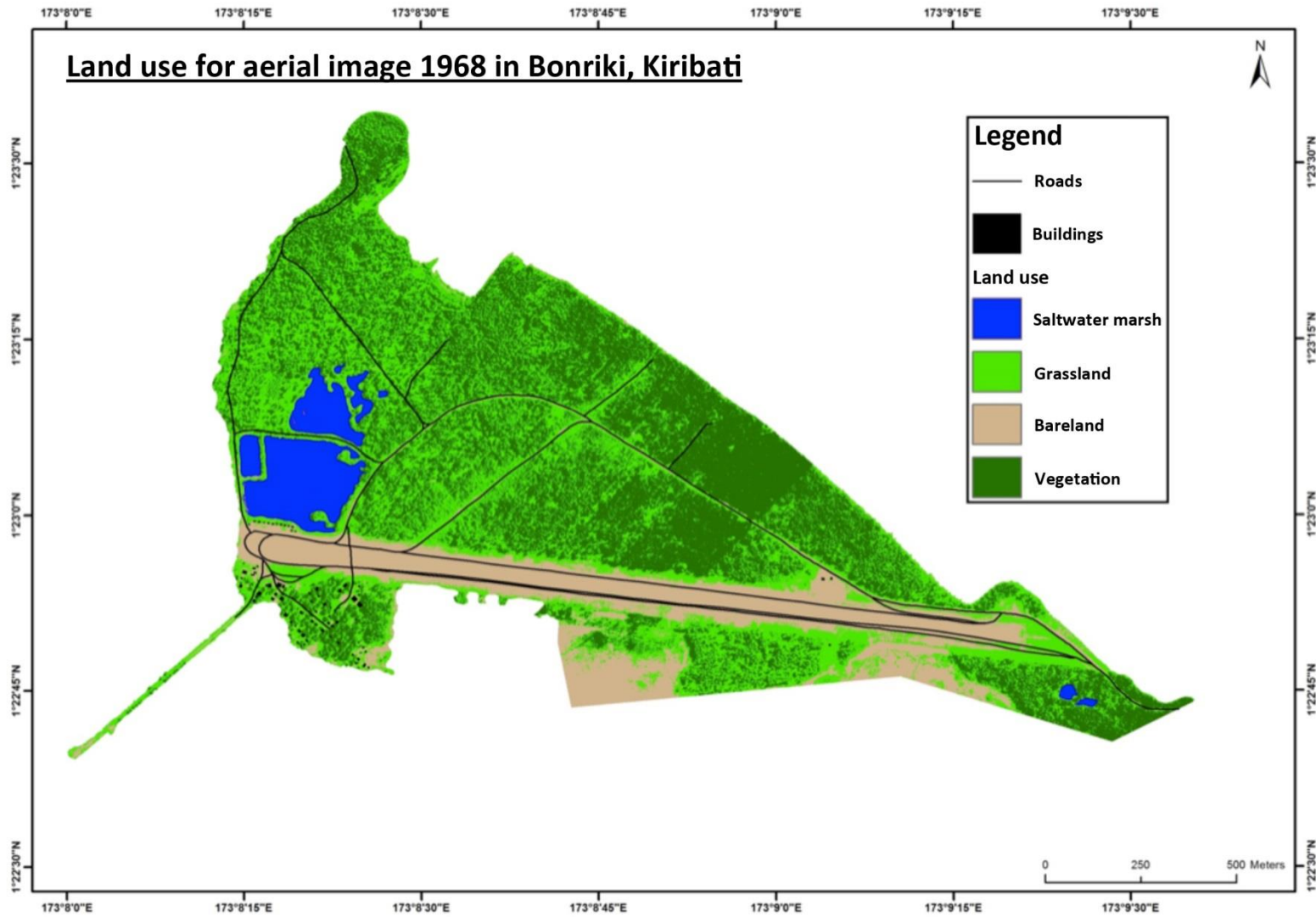


Figure 7: Land use classification for aerial image, 1968

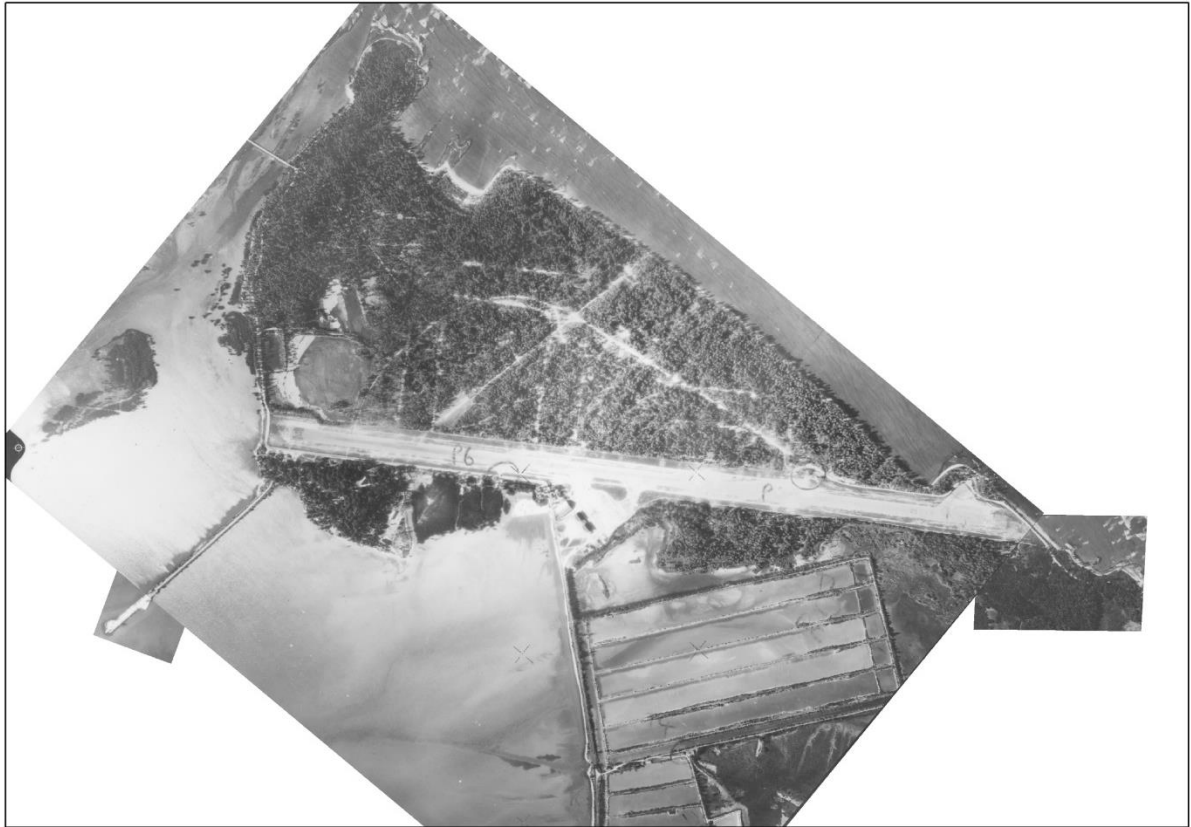


Figure 8: Geo-referenced aerial image, 1984 – used for land use classification

Three training samples were assigned for the 1984 aerial photograph: vegetation, saltwater marsh and bareland.

The image has only one band, which is not sufficient to differentiate between vegetation and grassland, so these were combined. Re-coding was carried out for saltwater marsh.

Table 10: Contingency error matrix for the aerial image, 1984

Classified data	Reference data (in pixels)			Row total
	Saltwater marsh	Vegetation	Bareland	
Saltwater marsh	806030	38562	15939	860531
Vegetation	71820	162583	0	234403
Bareland	2551	0	1393180	1395731
Column total	880401	201145	1409119	2490665

Table 11: Results of the accuracy assessment for the supervised classification: 1984 aerial image

Classification	Reference total	Classified total	Number correct	Producer's accuracy	User's accuracy
Background	4	4	4	100.00%	100.00%
Saltwater marsh	7	7	7	100.00%	100.00%
Bareland	20	26	19	95.00%	73.08%
Vegetation	69	63	62	89.86%	98.41%
Total	100	100	92		
Overall classification accuracy = 92.00%					

Table 12: Error matrix (in pixels) of the accuracy assessment for the supervised classification: 1984 aerial image

Classification	Background	Saltwater marsh	Bareland	Vegetation	Total
Background	4	0	0	0	4
Saltwater marsh	0	7	0	0	7
Bareland	0	0	19	7	26
Vegetation	0	0	1	62	63
Total	4	7	20	69	100

Table 13: Kappa statistics of the accuracy assessment for the supervised classification: 1984 aerial image

Classification	Kappa
Background	1.0000
Saltwater marsh	1.0000
Bareland	0.6635
Vegetation	0.9488
Overall kappa value = 0.8421	

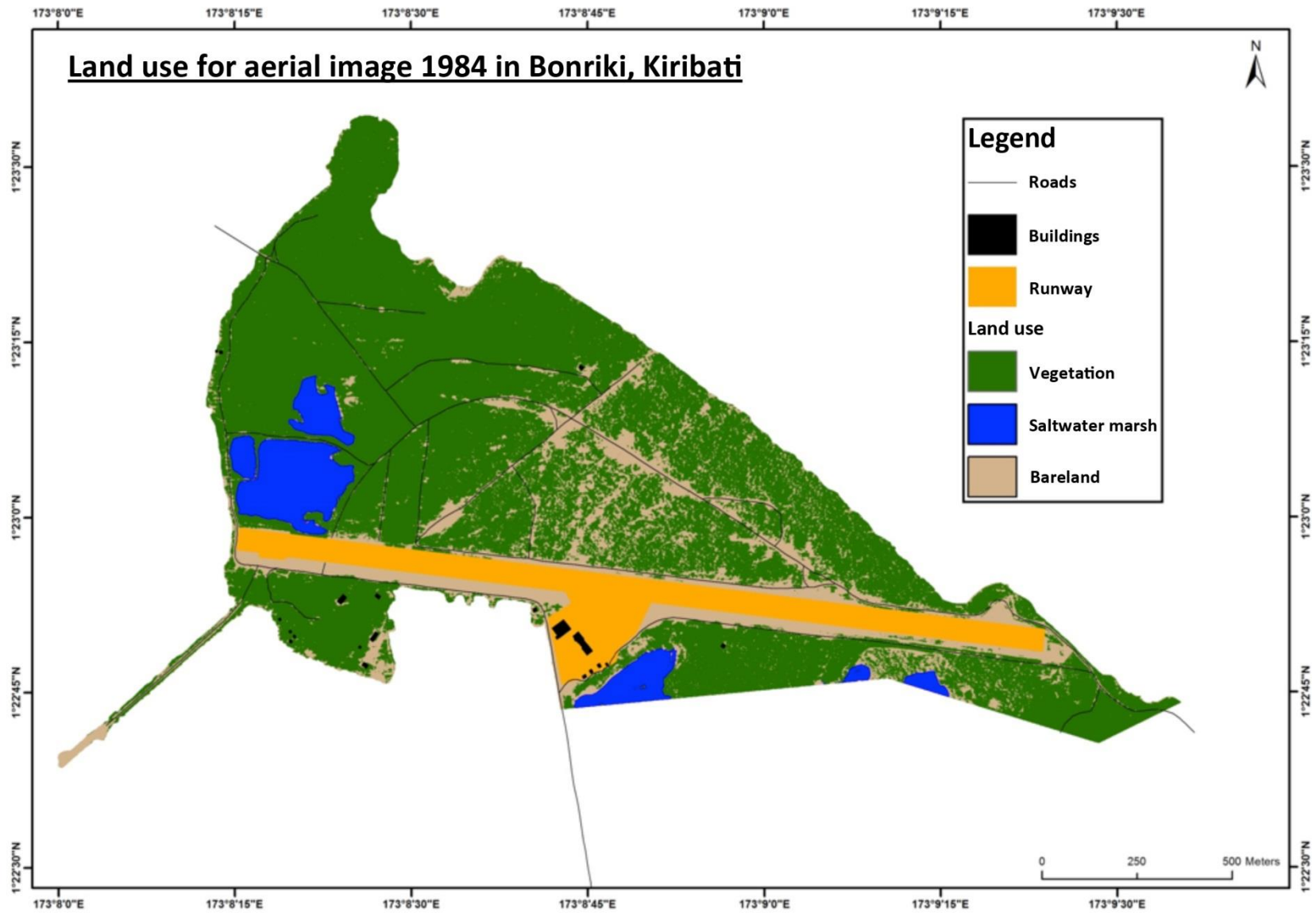


Figure 9: Land use classification for aerial image, 1984



Figure 10: Geo-referenced image, 1998 – used for land use classification

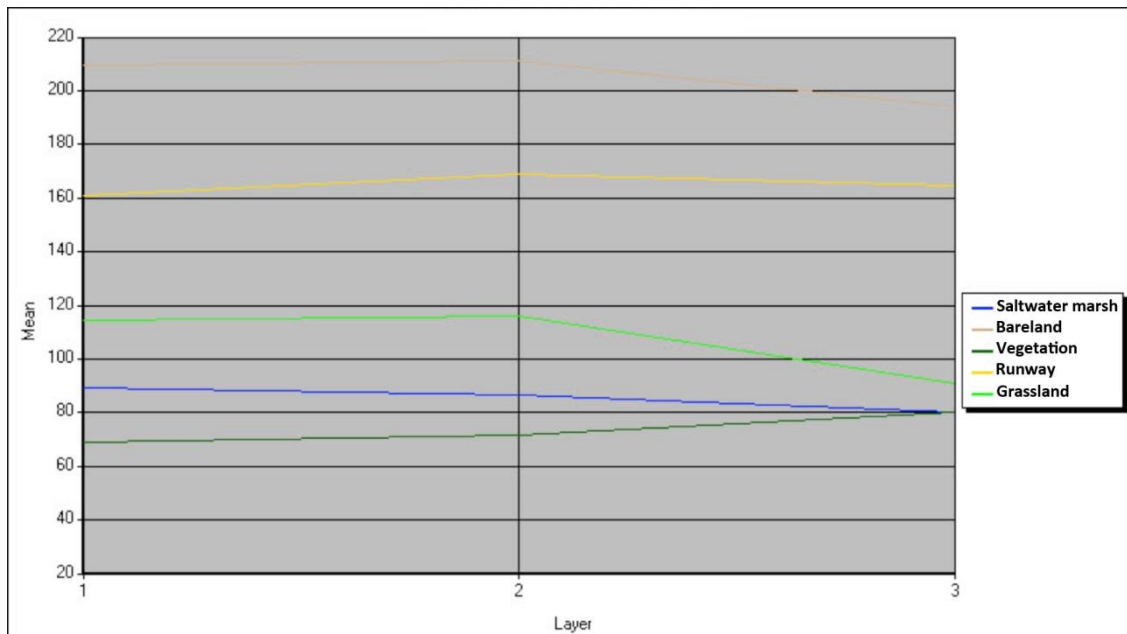


Figure 11: Signature Mean Plot for classifications in aerial image, 1998

Table 14: Contingency error matrix for the aerial image, 1998

Classified data	Reference data (in pixels)			
	Bareland	Vegetation	Grassland	Saltwater marsh
Bareland	33890	10	8	0
Vegetation	0	14283	100	303
Grassland	0	234	10858	0
Saltwater marsh	0	2544	0	22451
Column total	33890	17071	10966	22754

Table 15: Results of the accuracy assessment for the supervised classification: 1998 aerial image

Classification	Reference total	Classified total	Number correct	Producer's accuracy	User's accuracy
Background	5	3	3	-----	-----
Saltwater marsh	9	9	9	100.00%	100.00%
Bareland	19	18	18	94.74%	100.00%
Vegetation	31	35	30	96.77%	85.71%
Grassland	36	35	33	91.67%	94.29%
Total	100	100	93		
Overall classification accuracy = 93.00%					

Table 16: Error matrix (in pixels) of the accuracy assessment for the supervised classification: 1998 aerial image

Classification	Background	Saltwater marsh	Bareland	Vegetation	Grassland	Total
Background	3	0	0	0	0	3
Saltwater marsh	0	9	0	0	0	9
Bareland	0	0	18	0	0	18
Vegetation	2	0	0	30	3	35
Grassland	0	0	1	1	33	35
Total	5	9	19	30	36	100

Table 17: Kappa statistics of the accuracy assessment for the supervised classification: 1998 aerial image

Classification	Kappa
Background	1.0000
Saltwater marsh	1.0000
Bareland	1.0000
Vegetation	0.7930
Overall kappa value = 0.9030	

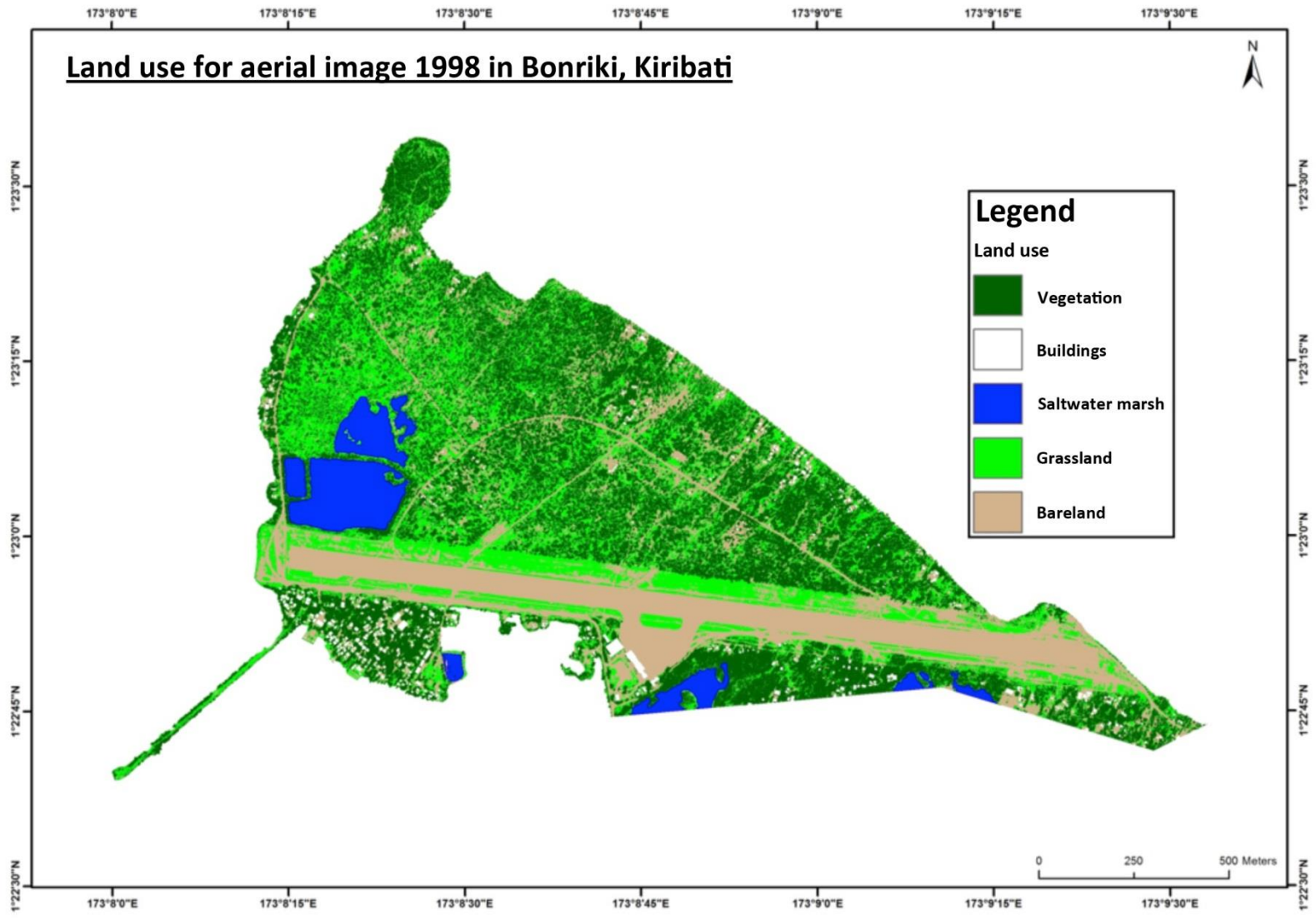


Figure 12: Land use classification for aerial image, 1998

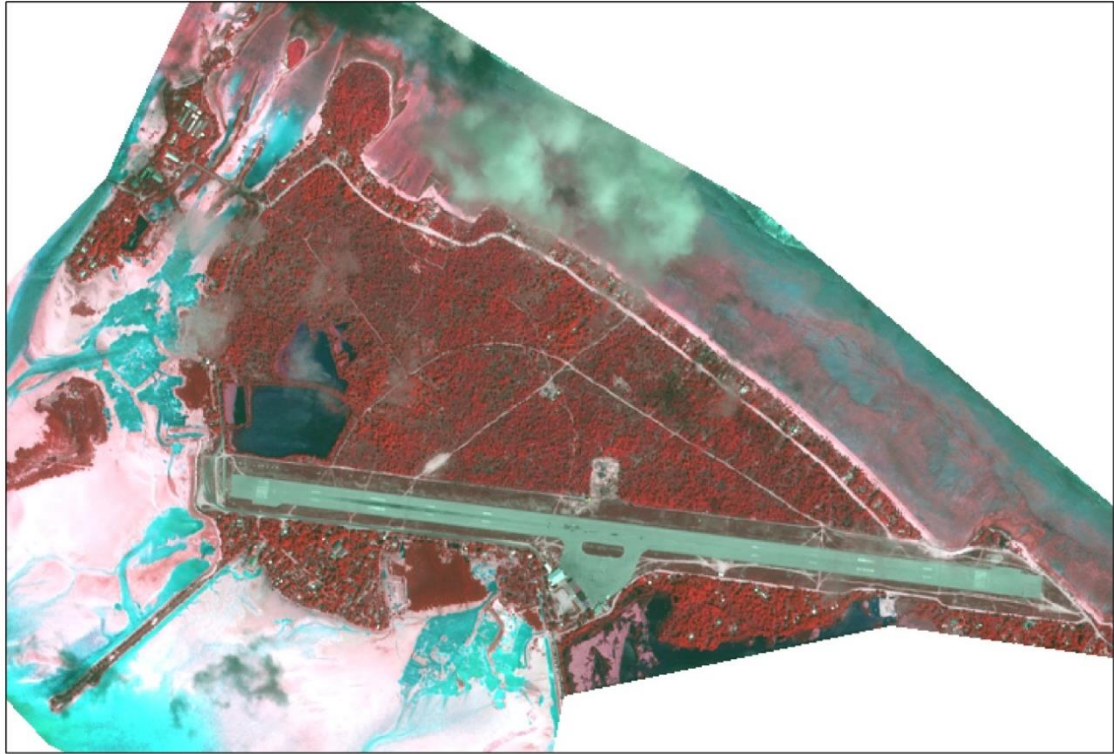


Figure 13: IKONOS image (false colour composite), 2003 – used for land use classification

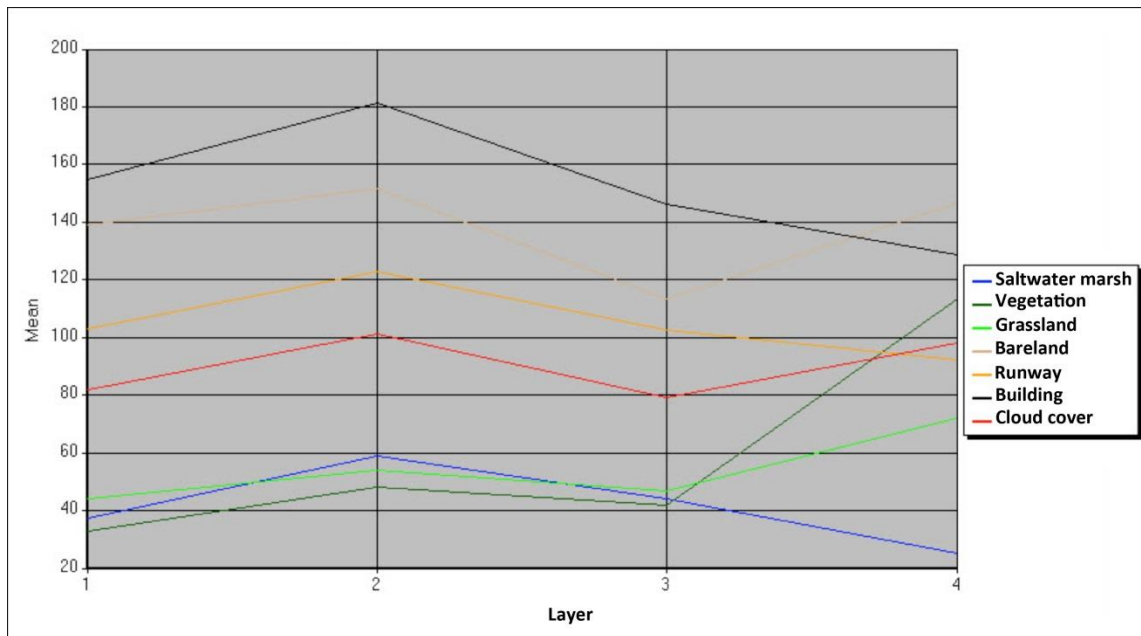


Figure 14: Signature Mean Plot for classifications in the IKONOS image, 2003

Table 18: Contingency error matrix for the IKONOS image, 2003

Reference data (in pixels)								
Classified data	Saltwater marsh	Vegetation	Grassland	Bareland	Runway	Building	Cloud cover	Row total
Saltwater marsh	2394	0	0	0	0	0	0	2394
Vegetation	0	91	12	1	63	0	5	172
Grassland	0	0	320	0	2	0	0	322
Bareland	0	1	0	262	41	0	3	307
Runway	0	1	0	0	8003	0	0	8004
Building	0	0	0	1	184	79	0	264
Cloud cover	6	0	0	2	21	0	402	431
Column total	2400	93	332	266	8314	79	410	11894

Table 19: Results of the accuracy assessment for the supervised classification: 2003 IKONOS image

Classification	Reference total	Classified total	Number correct	Producer's accuracy	User's accuracy
Vegetation	51	62	50	98.04%	80.65%
Grassland	18	12	10	55.56%	83.33%
Runway	3	3	3	100.00%	100.00%
Saltwater marsh	8	6	6	75.00%	100.00%
Cloud cover	1	1	1	100.00%	100.00%
Bareland	18	15	13	72.22%	86.67%
Building	1	1	1	100.00%	100.00%
Total	100	100	88		
Overall classification accuracy = 84.00%					

Table 20: Error matrix (in pixels) of the accuracy assessment for the supervised classification: 2003 IKONOS image

Classification	Vegetation	Grassland	Runway	Saltwater marsh	Cloud cover	Bareland	Building	Total
Vegetation	50	8	0	0	0	4	0	62
Grassland	1	10	0	0	0	1	0	12
Runway	0	0	3	0	0	0	0	3
Saltwater marsh	0	0	0	6	0	0	0	6
Cloud cover	0	0	0	0	1	0	0	1
Bareland	0	0	0	2	0	13	0	15
Building	0	0	0	0	0	0	1	1
Total	51	18	3	8	1	18	1	100

Table 21: Kappa statistics of the accuracy assessment for the supervised classification: 2003 IKONOS image

Classification	Kappa
Vegetation	0.6050
Grassland	0.7967
Runway	1.0000
Saltwater marsh	1.0000
Cloud cover	1.0000
Bareland	0.8374
Building	1.0000
Overall kappa value = 0.7457	

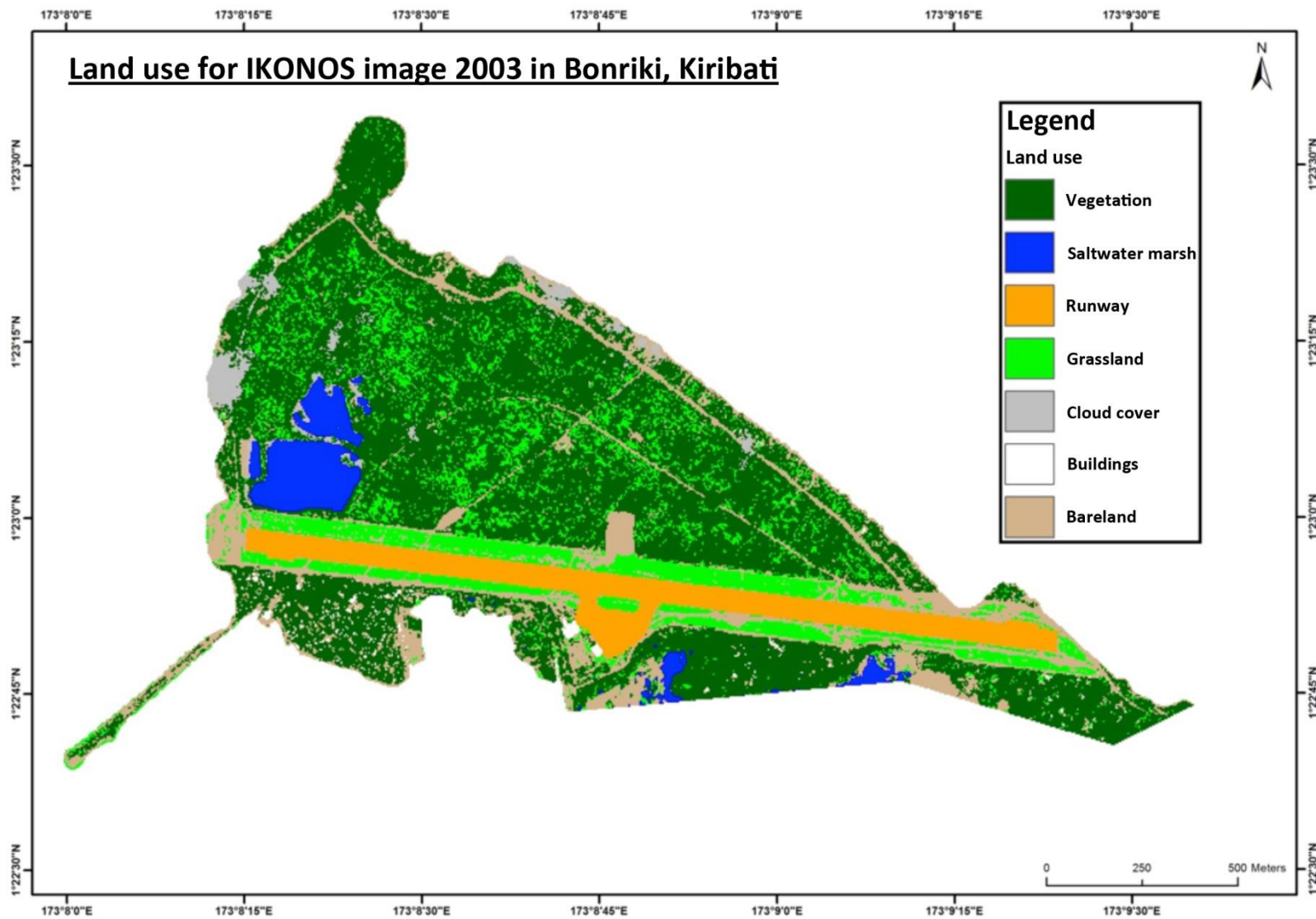


Figure 15: Land use classification for the IKONOS image, 2003



Figure 16: Quick Bird PS image, 2007 – used for land use classification

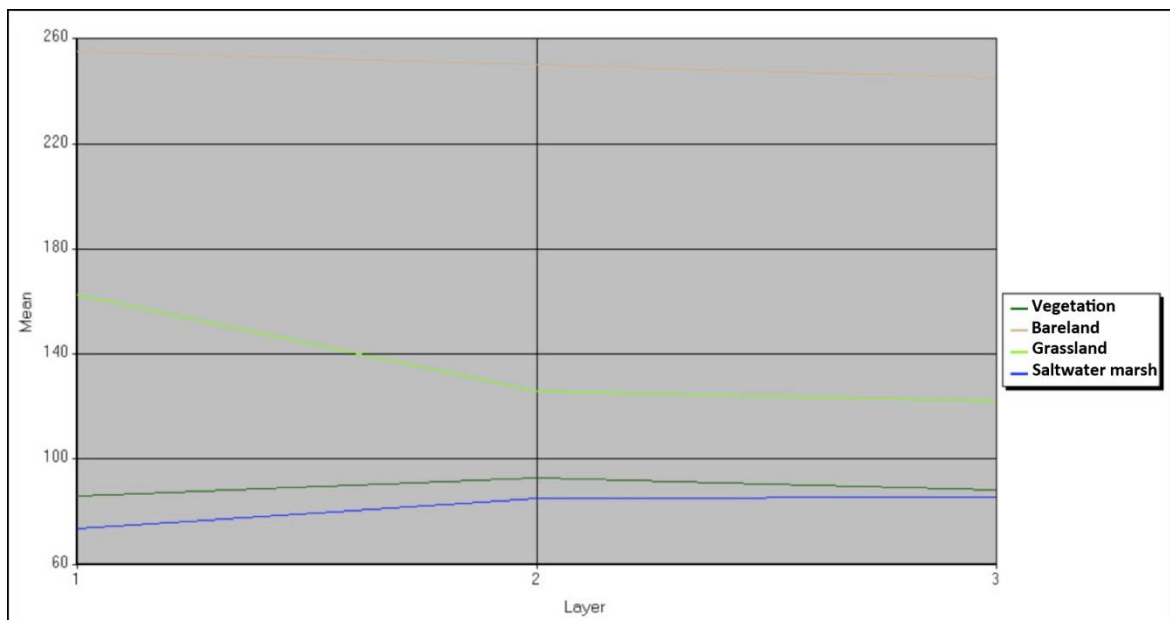


Figure 17: Signature Mean Plot for classifications in Quick Bird PS, 2007

Table 22: Contingency error matrix for the Quick Bird PS image, 2007

Reference data (in pixels)				
Classified data	Vegetation	Bareland	Grassland	Saltwater marsh
Vegetation	18167	35	2	906
Bareland	0	95090	3	0
Grassland	1	753	27785	0
Saltwater marsh	1911	0	0	8773
Column total	20079	95878	27790	9679

Table 23: Results of the accuracy assessment for the supervised classification: 2007 Quick Bird PS image

Classification	Reference total	Classified total	Number correct	Producer's accuracy	User's accuracy
Background	2	4	2		
Saltwater marsh	8	8	8	100.00%	100.00%
Bareland	10	9	9	90.00%	100.00%
Vegetation	48	46	46	95.83%	100.00%
Grassland	32	33	32	100.00%	96.97%
Total	100	100	97		
Overall classification accuracy = 97.00%					

Table 24: Error matrix (in pixels) of the accuracy assessment for the supervised classification: 2007 Quick Bird PS image

Classification	Background	Saltwater marsh	Bareland	Vegetation	Grassland	Total
Background	2	0	1	1	0	4
Saltwater marsh	0	8	0	0	0	8
Bareland	0	0	9	0	0	9
Vegetation	0	0	0	46	0	46
Grassland	0	0	0	1	32	33
Total	2	8	10	48	32	100

Table 25: Kappa statistics of the accuracy assessment for the supervised classification: 2007 Quick Bird PS image

Classification	Kappa
Background	0.4898
Saltwater marsh	1.0000
Bareland	1.0000
Vegetation	1.0000
Grassland	0.9554
Overall kappa value = 0.9544	

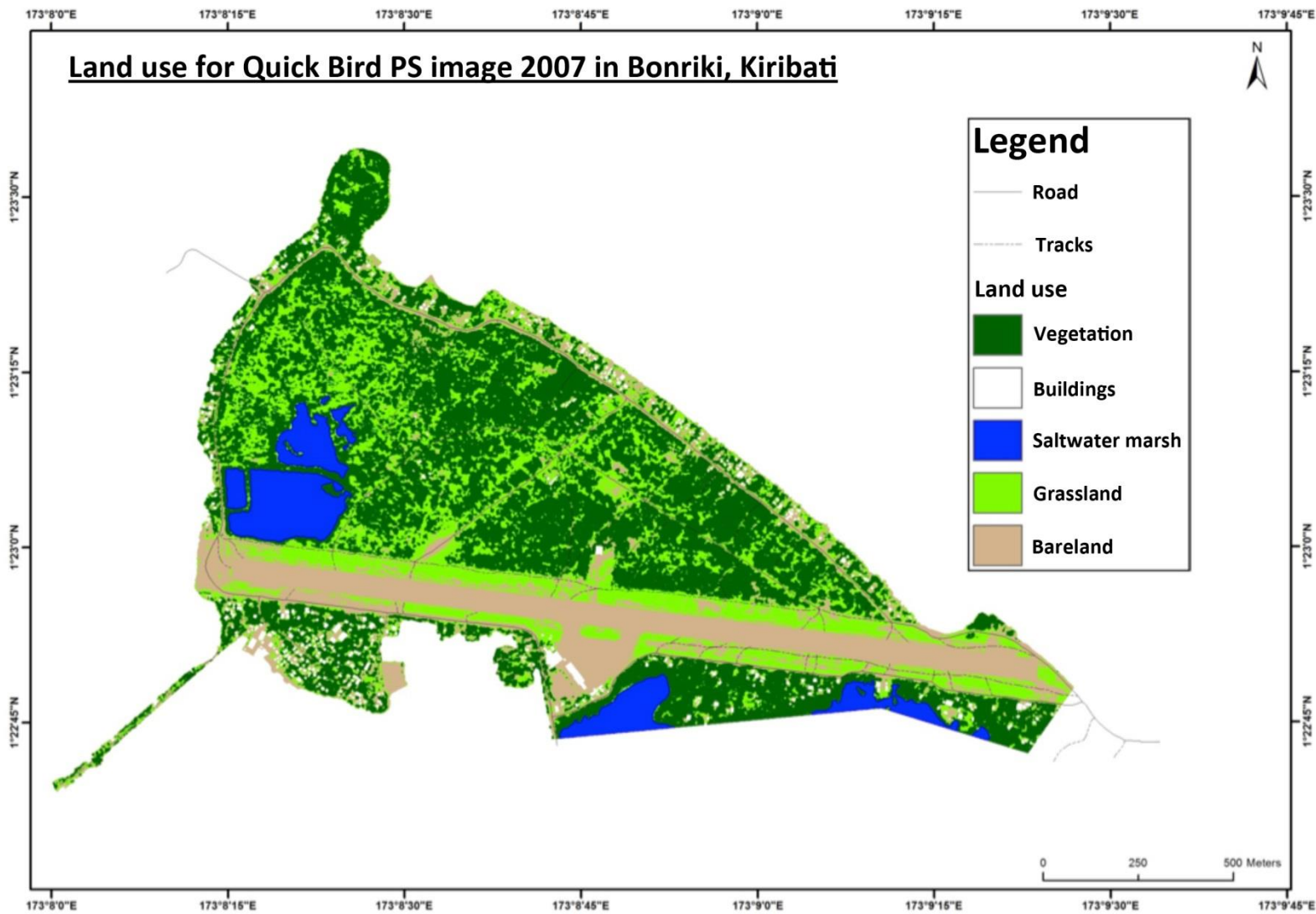


Figure 18: Land use classification for Quick Bird PS image, 2007

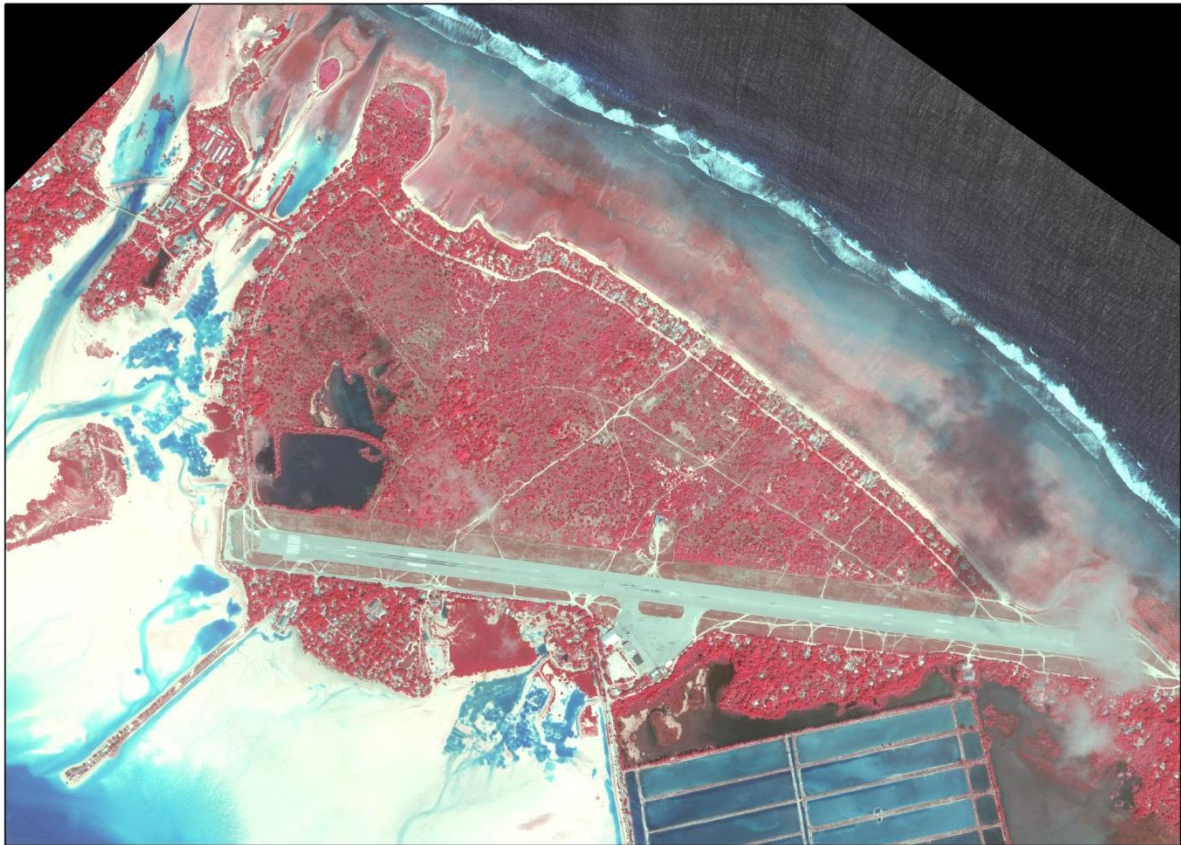


Figure 19: Geo-Eye image (false colour composite), 2012 – used for land use classification

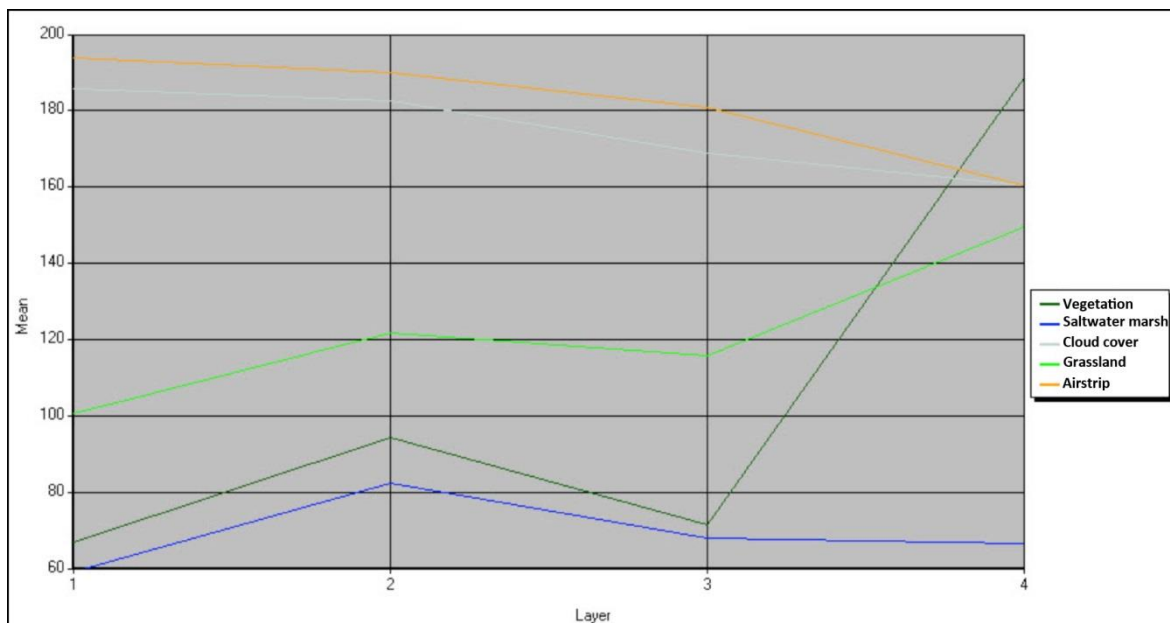


Figure 20: Signature Mean Plot for classifications used in Geo-Eye, 2012

Table 26: Contingency error matrix (in pixels) for the Geo-Eye image, 2012

Classified data	Reference data (in pixels)							Row total
	Saltwater marsh	Vegetation	Grassland	Bareland	Runway	Building	Cloud cover	
Saltwater marsh	2394	0	0	0	0	0	0	2394
Vegetation	0	91	12	1	63	0	5	172
Grassland	0	0	320	0	2	0	0	322
Bareland	0	1	0	262	41	0	3	307
Runway	0	1	0	0	8003	0	0	8004
Building	0	0	0	1	184	79	0	264
Cloud cover	6	0	0	2	21	0	402	431
Column total	2400	93	332	266	8314	79	410	11894

Table 27: Results of the accuracy assessment for the supervised classification: 2012 Geo-Eye image

Classification	Reference total	Classified total	Number correct	Producer's accuracy	User's accuracy
Background	4	5	4	-----	-----
Runway	3	3	3	100.00%	100.00%
Cloud cover	2	2	2	100.00%	100.00%
Saltwater marsh	8	7	7	87.50%	100.00%
Vegetation	43	45	42	97.67%	93.33%
Grassland	33	33	30	90.91%	90.91%
Bareland	7	5	5	71.43%	100.00%
Total	100	100	93		
Overall classification accuracy = 93.00%					

Table 28: Error matrix (in pixels) of the accuracy assessment for the supervised classification: 2012 Geo-Eye image

Classification	Background	Runway	Cloud cover	Saltwater marsh	Vegetation	Grassland	Bareland	Total
Background	4	0	0	0	1	4	0	5
Runway	0	3	0	0	0	0	0	3
Cloud cover	0	0	2	0	0	0	0	2
Saltwater marsh	0	0	0	7	0	0	0	7
Vegetation	0	0	0	0	42	3	0	45
Grassland	0	0	0	1	0	30	0	33
Bareland	0	0	0	0	0	0	5	5
Total	4	3	2	8	43	33	7	100

Table 29: Kappa statistics of the accuracy assessment for the supervised classification: 2012 Geo-Eye image

Classification	Kappa
Background	0.7917
Runway	1.0000
Cloud cover	1.0000
Saltwater marsh	1.0000
Vegetation	0.8830
Grassland	0.8643
Bareland	1.0000
Overall kappa value = 0.8978	

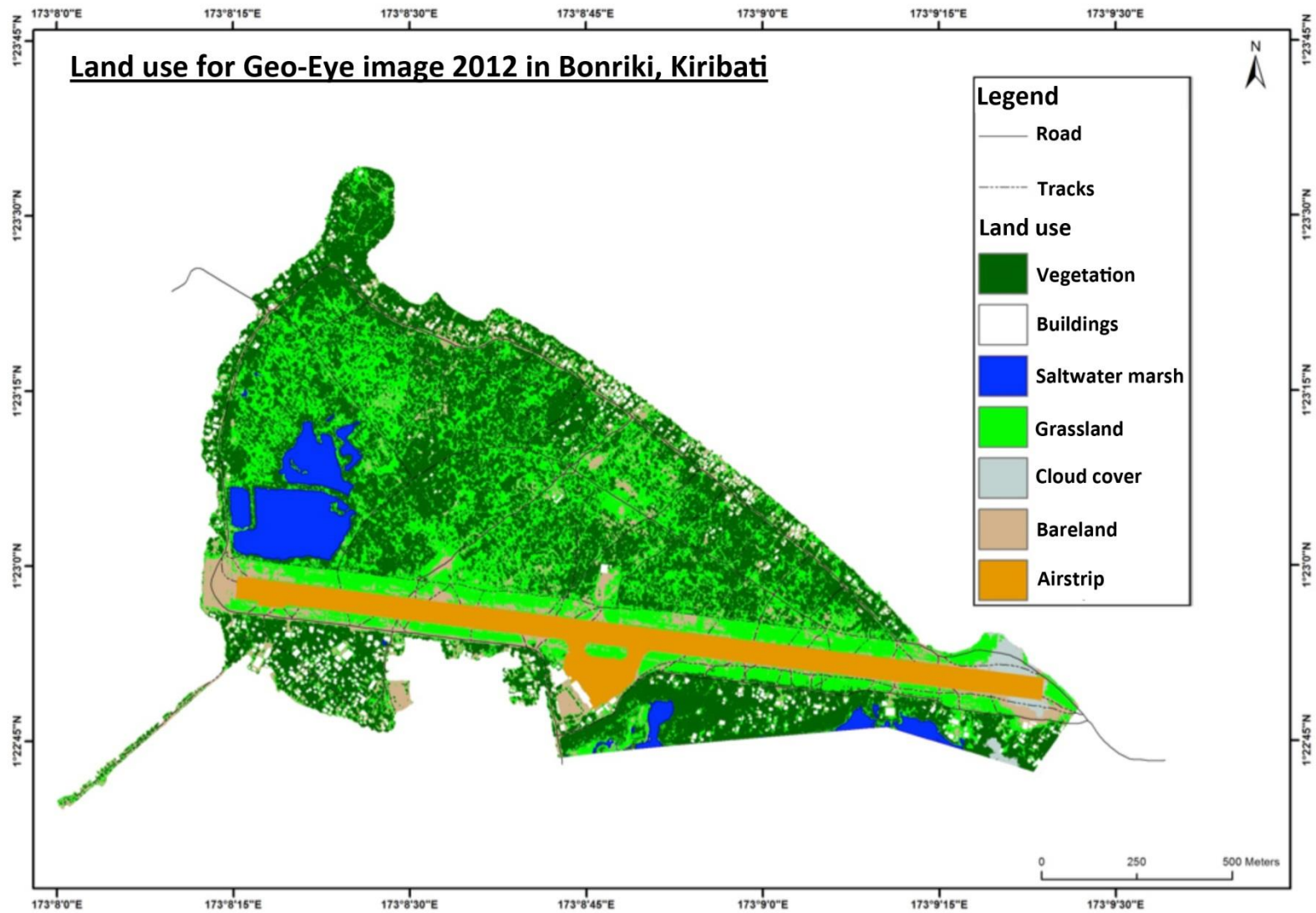


Figure 21: Land use classification for Geo-Eye image, 2012

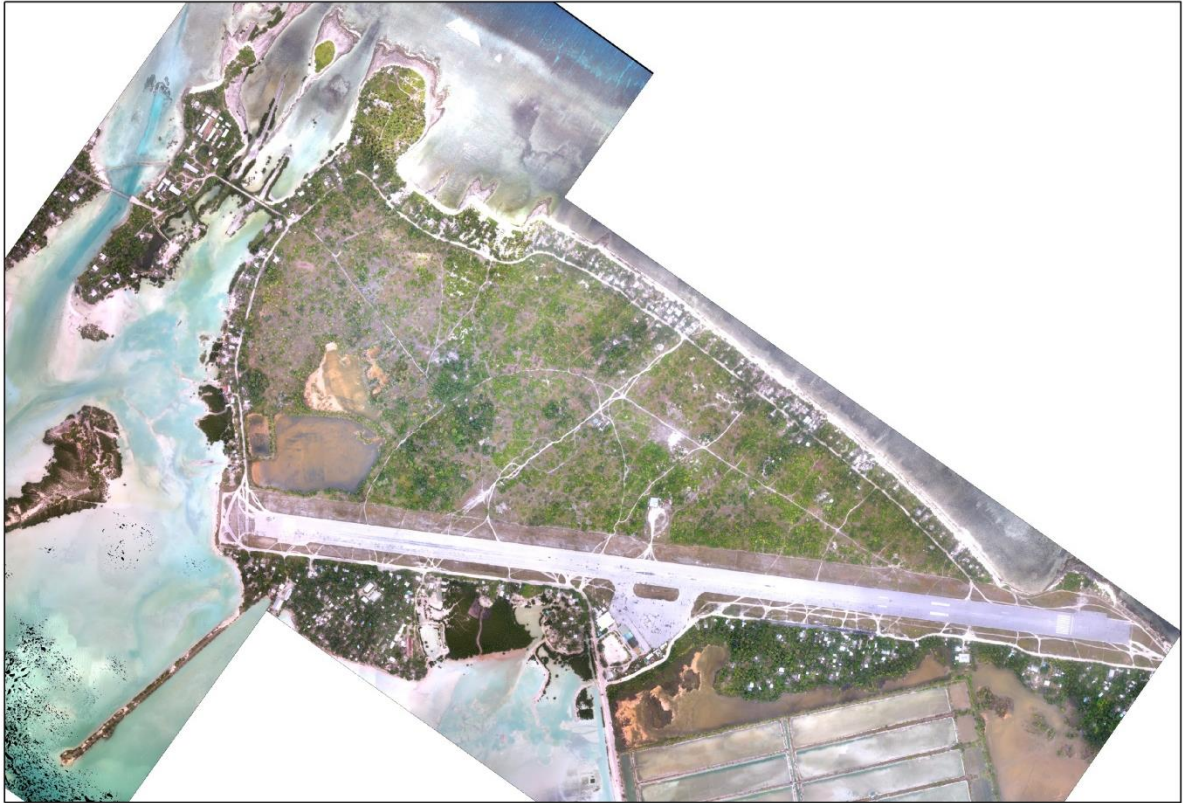


Figure 22: UAV Ortho-photo, 2014 – used for land use classification

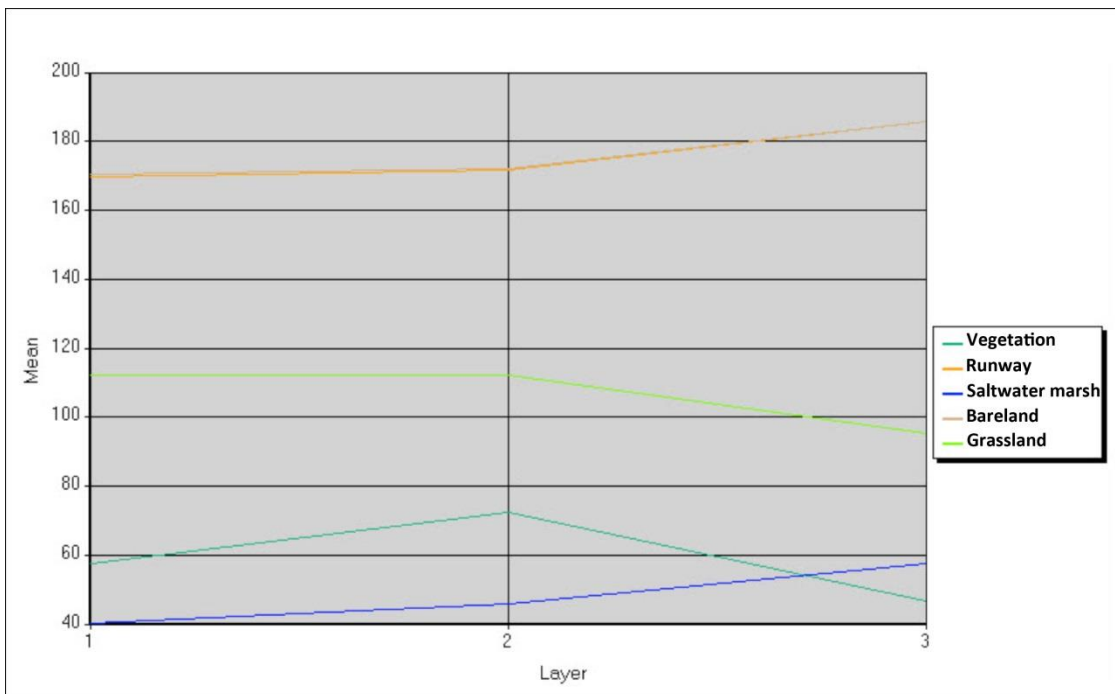


Figure 23: Signature Mean Plot for classifications used in the UAV Ortho-photo

Table 30: Contingency error matrix for the UAV Ortho-photo, 2014

Reference data (in pixels)						
Classified data	Bareland	Vegetation	Runway	Grassland	Saltwater Marsh	Row total
Bareland	354296	0	2470	18	0	356784
Vegetation	491	123734	2056	189	70	124014
Runway	226	0	1312704	0	0	1312930
Grassland	1023	3	932	274259	0	276217
Saltwater marsh	0	0	5	0	6936	6941
Column total	356036	123737	1318167	274466	7006	2079412

Table 31: Results of the accuracy assessment for the supervised classification: 2014 UAV Ortho-photo

Classification	Reference total	Classified total	Number correct	Producer's accuracy	User's accuracy
Background	7	7	7	-----	-----
Saltwater marsh	9	9	9	100.00%	100.00%
Runway	3	3	3	100.00%	100.00%
Grassland	25	24	24	96.00%	100.00%
Bareland	19	17	17	89.47%	100.00%
Vegetation	37	40	37		
Total	100	100	97		
Overall classification accuracy = 97.00%					

Table 32: Error matrix (in pixels) of the accuracy assessment for the supervised classification: 2014 UAV Ortho-photo

Classification	Background	Saltwater marsh	Runway	Grassland	Bareland	Vegetation	Total
Background	7	0	0	0	0	0	7
Saltwater marsh	0	9	0	0	0	0	9
Runway	0	0	3	0	0	0	3
Grassland	0	0	0	24	0	0	24
Bareland	0	0	0	0	17	0	17
Vegetation	0	0	0	1	2	37	40
Total	7	9	3	25	19	37	100

Table 33: Kappa statistics of the accuracy assessment for the supervised classification: 2014 UAV Ortho-photo

Classification	Kappa
Background	1.0000
Saltwater marsh	1.0000
Runway	1.0000
Grassland	1.0000
Bareland	1.0000
Vegetation	0.8810
Overall kappa value = 0.9598	

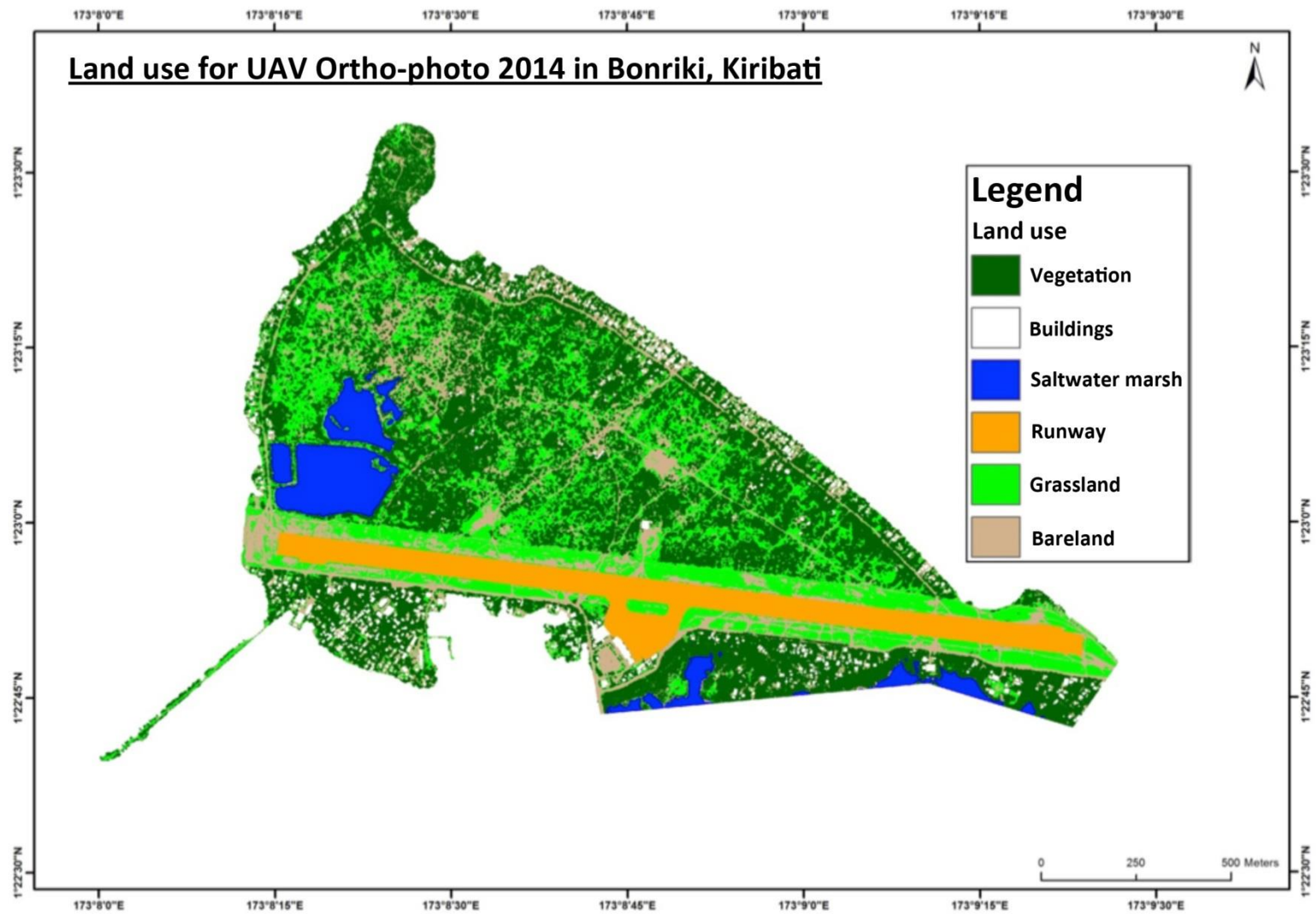


Figure 24: Land use classification for UAV Ortho-photo, 2014

4. Analysis

Table 34: Area calculation of classified categories for images

Classified data	1943			1968			1984			1998		
	Pixel count	Area (sq.m)	(%)	Pixel count	Area (sq.m)	(%)	Pixel count	Area (sq.m)	(%)	Pixel count	Area (sq.m)	(%)
Vegetation	780689	803861	46.81	7860648	707458	40.50	3286986	1183315	66.70	10625329	664083	38.26
Bareland	813448	829364	48.29	3450623	310556	17.78	1341862	483070	27.23	7218761	451173	25.99
Saltwater marsh	83960	83960	4.88	0	83245	4.76	289519	104227	5.87	1770172	110636	6.37
Grassland	---	---		7168019	645122	36.94	---	---		7698736	481171	27.72
Buildings					3782	0.21		3381	0.19		28439	1.63
Total		1717185	100		1746383	100		1773993	100		1735502	100

Classified data	2003			2007			2012			2014		
	Pixel count	Area (sq.m)	(%)	Pixel count	Area (sq.m)	(%)	Pixel count	Area (sq.m)	(%)	Pixel count	Area (sq.m)	(%)
Vegetation	60322	958960	54.50	2232190	803588	46.07	3024937	756234	43.55	76341519	763415	44.31
Bareland	25904	391072	22.22	1008106	362918	20.81	1345098	336275	19.36	41918984	419190	24.33
Saltwater marsh	4748	75152	4.27	306157	110217	6.31	351020	87755	5.05	9429476	94295	5.47
Grassland	17936	284432	16.16	1209788	435524	24.97	1972372	493093	28.39	39571433	395714	22.96
Buildings	722	11552	0.65		31689	1.81		48929	2.81	5	50152	2.91
Cloud cover	2566	38192	2.17				56353	14088	0.81			
Total		1759360	100		1743936	100		1736374	100		1722766	100

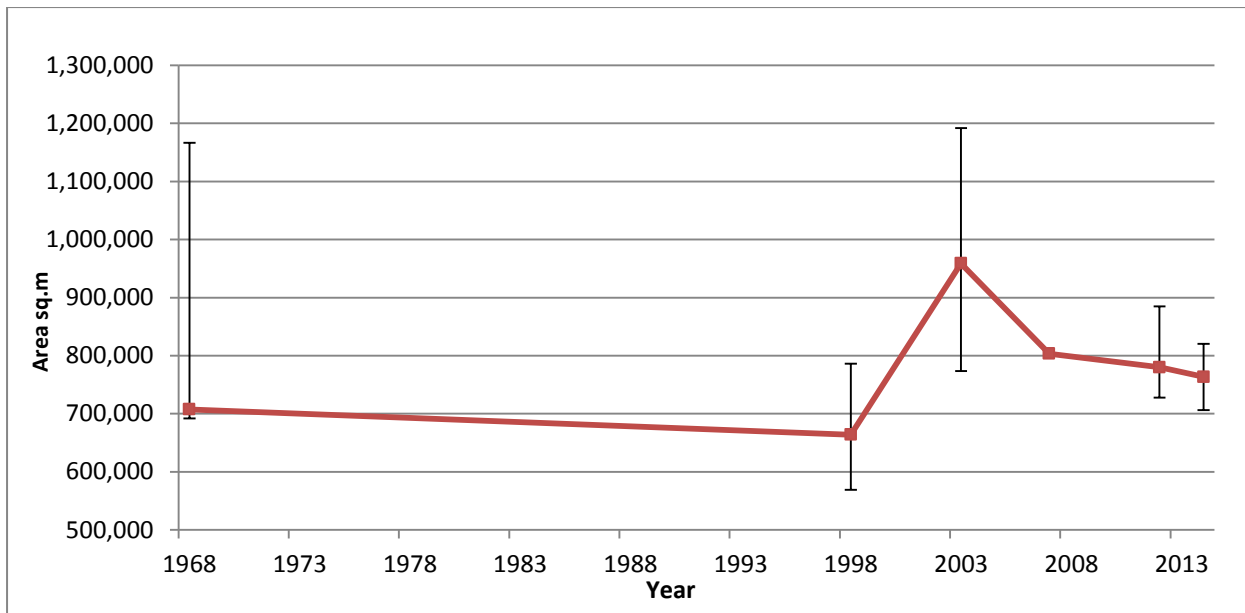


Figure 25: Vegetation area changes from 1968 to 2014

Note: Vertical bars at data points represent error bars derived from producer and user accuracy.

Figure 25 shows the historical fluctuation of vegetation area over Bonriki since 1968. Given the high degree of uncertainty in the classification of vegetation areas, especially for 1968, 1998 and 2003, it is not possible to draw conclusions about trends with confidence.

Vegetation area for 1968 had a high level of error, as shown in the error matrix in Table 7, where the overall producer's accuracy was 29.17%. This was due to the image being one band black and white, providing very little information to confidently differentiate between grassland and vegetation. While it is likely that there was a decrease in vegetation from 1968 to 1998, such a conclusion cannot be reached with the available data. Image classification shows an increase in vegetation from 1998 to 2003. However, the uncertainty attributed to the classification of vegetation for 1998 and 2003 makes it difficult to quantify the increase with confidence. Vegetation has gradually decreased, from 2003 to 2014, possibly due to increasing population, which is shown in Figure 29 as a near exponential growth in buildings count. This build up has in turn reduced bareland cover over this period, as shown in Table 34.

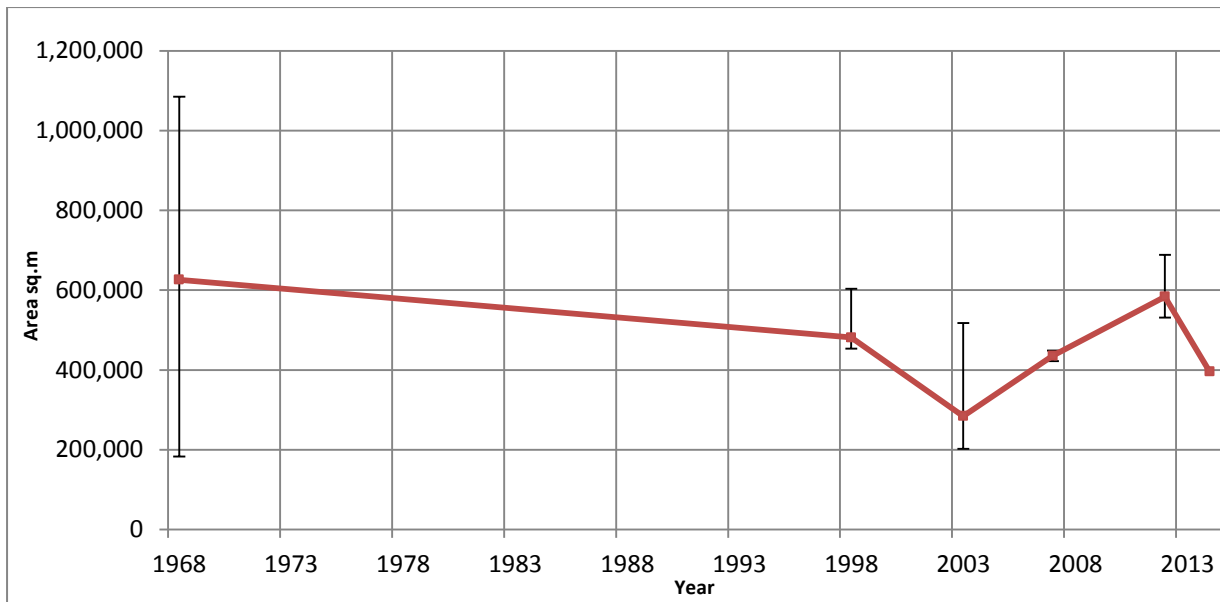


Figure 26: Grassland area changes from 1968 to 2014

Note: Vertical bars at data points represent error bars derived from producer and user accuracy.

Figure 26 shows the historical fluctuation of grassland area over Bonriki since 1968. Given high levels of uncertainty in the classification of grassland area, especially for the years 1968, 1998 and 2003, it is not possible to draw conclusions with confidence about trends in grassland area changes.

In 1968 grassland area indicated by the image classification has a high level of uncertainty, which prevents any conclusion to be drawn from this data. An increase in grassland area is observed from 2003 to 2012 but it is difficult to correlate this to an unusually high average monthly rainfall over that period (Figure 30). 2014 indicated a decrease in grassland, again, this may be due to lower rainfall and a particularly dry season experienced in that year.

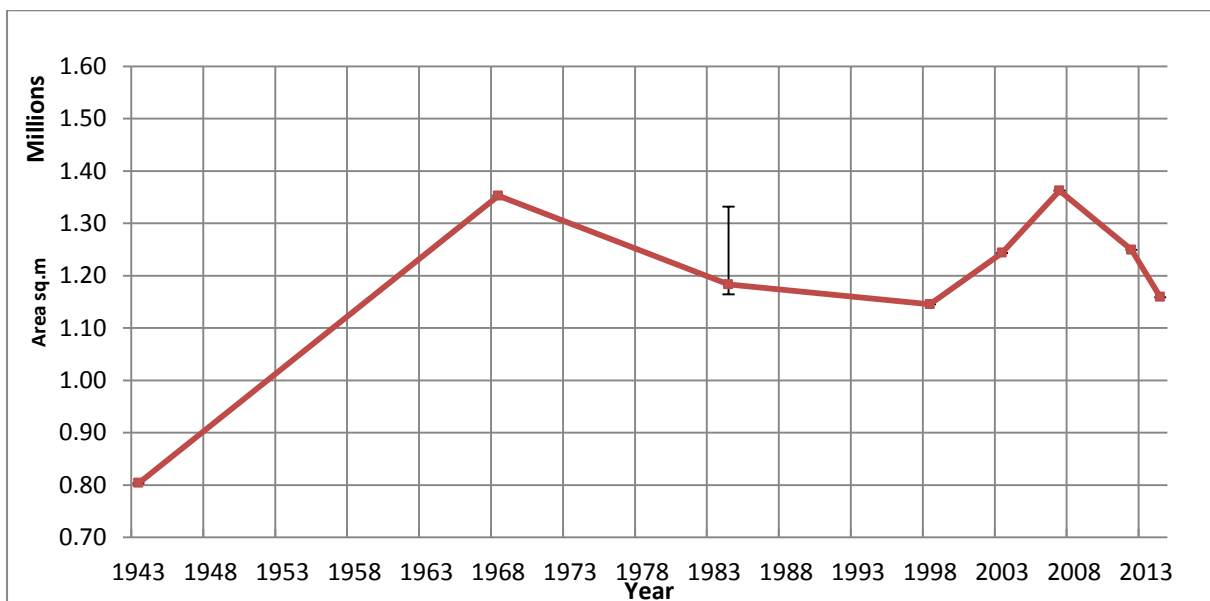


Figure 27: Combined vegetation and grassland area changes from 1943 to 2014

Note: Vertical bars at data points represent error bars derived from producer and user accuracy. Only

Change detection in Figure 27 combines vegetation and grassland classifications from 1943 to 2014, in an attempt to reduce the uncertainties and better visualise overall changes in vegetation. The graph shows that after the initial re-vegetation following the disturbance after World War II, the vegetation cover has been relatively stable. A decline in recent years since 2008 is also decetable.

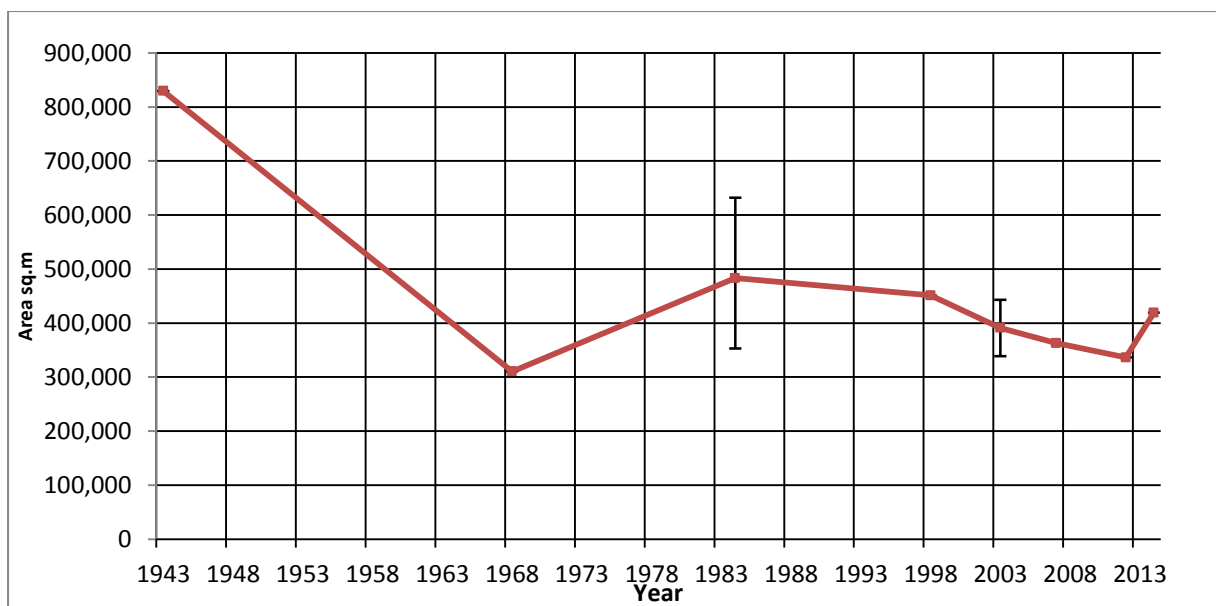


Figure 28: Bareland (runway) area changes from 1943 to 2014

Note: Vertical bars at data points represent error bars derived from producer and user accuracy.

As shown in Figure 27 and Figure 28, the main change in land cover occurred between 1943 and 1968. In 1943, during the Second World War, the United States Navy drastically changed the landscape of Bonriki, building two runways for military purposes. Consequently, the area of bareland in 1943 was approximately twice as large as it is today. There was a substantial reduction in bareland between 1943 and 1968, from 48.27% to 17.78% (these and subsequent percentages were derived from Table 34), which indicates vegetation re-growth on the former runway areas. Similarly, Figure 27 shows an increase in vegetation/grassland between 1943 and 1968, to 30.64% of land area. The 1984 image (Figure 8) evidences infrastructure development that occurred on Bonriki from 1968, leading to an increase in bareland to 27.23% of land area as shown in Table 34), and a decrease in vegetation/grassland coverage of 10.74%. In the early 1980s, Bonriki underwent large land reclamation, with the construction of a causeway, the airport and an expansion of the road network (Bishop 2011). From 1984, development (including land reclamation) and increased population resulted in a decrease in bareland until 2012. From 2012 to 2014, the increase in bareland area corresponding with the decrease in vegetation/grassland is likely to be explained by the dry season experienced in 2014.

The error bars in the figures highlight the uncertainty as calculated in the error matrix. Figure 28 indicates high uncertainty for 1984 and 2003. Other limitations inherent in the baseline data include cloud cover and missing near infra-red information. The near infra-red band, which is commonly used to differentiate bareland and grassland/vegetation, was only present in the 2003 and 2012 images. While error matrices can show that a satisfactory classification of bareland can be achieved using Red, Green, Blue information alone, error matrices do not reflect errors in areas where the user cannot differentiate between grassland and bareland. This is well illustrated for the 1998 image (Figure 10). The rainfall recorded in June 2014 was a below-average 47.4 mm, which led to the grass areas drying. The discolouration of the grassland area evident adjacent to the airport does not

enable the manual identification of grassland and bareland. Accordingly, these areas could not be included in the accuracy test.

There were no significant changes indicated in the area of saltwater marsh between 1943 and 2014. The changes, ranging from 1% to 2%, as shown in Table 34.

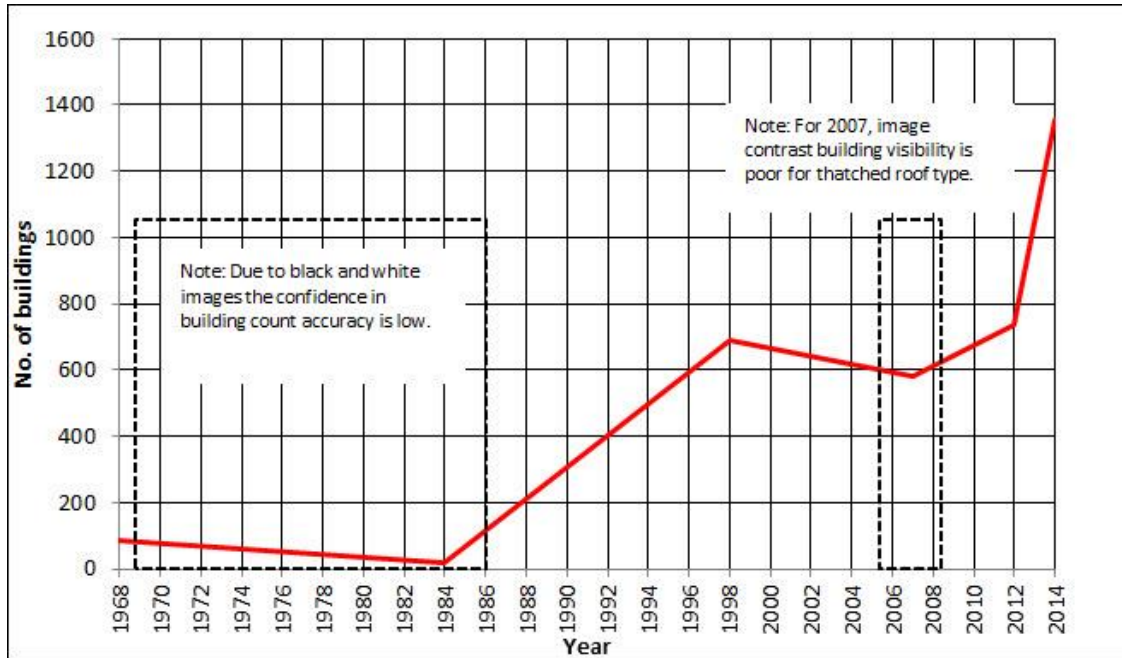


Figure 29: Buildings count changes from 1968 to 2014

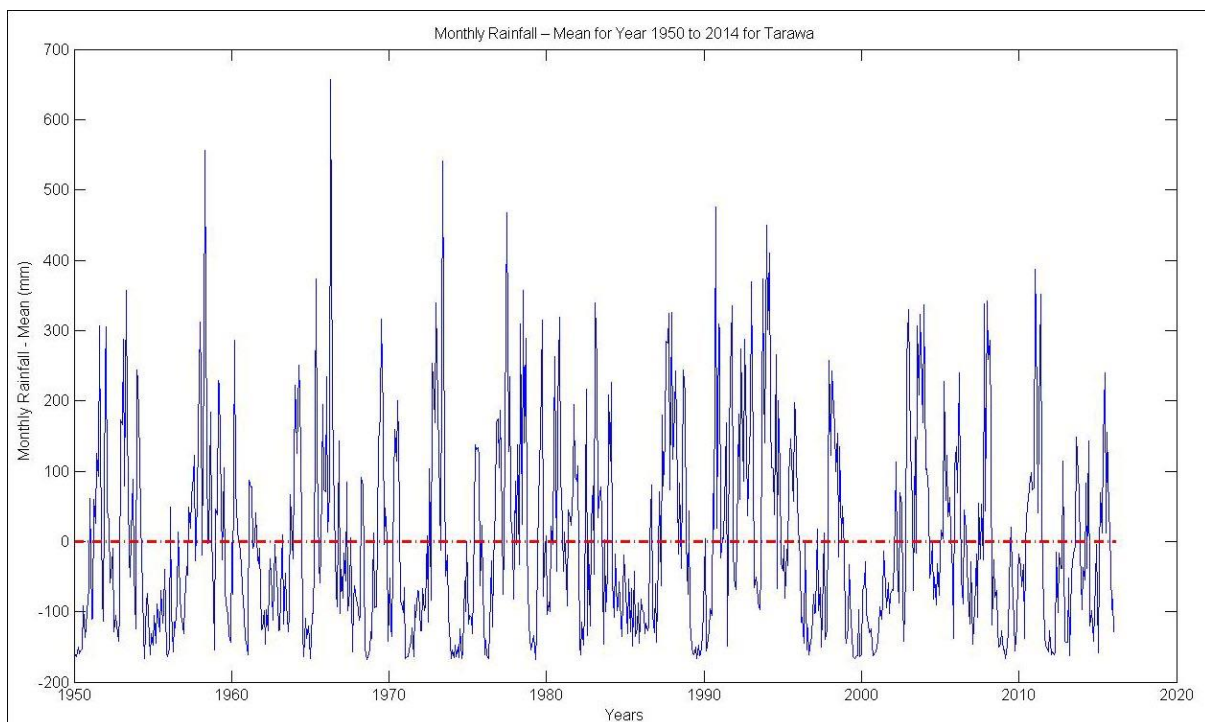


Figure 30: Monthly Tarawa rainfall – annual mean, 1950 to 2014

5. Conclusion

The classification methodology provides a satisfactory result, achieving an overall accuracy of 82% to 97%. Kappa statistics range from 0.84 to 0.95, except for the 1968 and 2003 images, which had lower kappa values, of 0.72 and 0.74, respectively. The low kappa value calculated for the 1968 image is due to the inclusion of grassland as a classification. The information provided by the black and white aerial image does not provide sufficient information to confidently differentiate vegetation and grassland classifications, in turn, creating an high matrix error. The low kappa value for the 2003 IKONOS image can be explained by the relatively low image resolution (4 meters), which resulted in a relatively low 55.56% producer accuracy for grassland. A kappa value greater than 0.8 represents a strong agreement and, accordingly, a good classification.

In land use/land cover analysis it is important to have a near infra-red spectral band to enable the detection of vegetation/grassland changes. Aerial images from 1943 to 1984 had only one spectral band, while the images from 1998 to 2014 had three bands (Red, Green, Blue). Near infra-red bands were only available in the 2003 and 2012 images. In order to achieve more accurate classifications it is necessary to separate the different classifications through identifying their spectral signatures in historical aerial images which have only one spectral band. Overall, good levels of accuracy were achieved with the one-band images in this study.

In order to improve classification, ground truthing is also very important. In this study, ground truthing was possible only for the 2014 UAV Aerial-photo. For the aerial images from 1968 to 1984, there is no metadata available on date of acquisition of imagery in order to compare with rainfall data to determine changes. However, using remote sensing enables the extraction of data on LULC changes over a period of time, but it does not explain the reasons for changes observed. Further investigation should be carried out to determine other factors (other than rainfall and building construction) that have affected the LULC, such as soil analysis and saltwater intrusion.

6. References

Australian Bureau of Meteorology and CSIRO. 2014. Climate variability, extremes and change in the western tropical Pacific: new Science and updated country reports. In: Pacific-Australia Climate Change Science and Adaptation Planning Program Technical Report. Melbourne, Australia. p. 113-127.

Jonathan M., Meirelles M.S.P., Berroir J.P. and Herlin I. 2007. Regional scale land use/land cover classification using temporal series of modis data. Revista Brasileira de Cartografia. 59. p. 1-7. sal.

KNSO and SPC 2012, Kiribati 2010 census. Volume 2, Analytical report. Kiribati National Statistics Office and the Secretariat of the Pacific Community Statistics for Development Program

Bishop A., Burhan I., Lowen T. and Snow Z.M S. 2011. South Tarawa General Land Use Plan. University of Melbourne Project.



CONTACT DETAILS
Secretariat of the Pacific Community

SPC Headquarters
BP D5,
98848 Noumea Cedex,
New Caledonia
Telephone: +687 26 20 00
Fax: +687 26 38 18

SPC Suva Regional Office
Private Mail Bag,
Suva,
Fiji,
Telephone: +679 337 0733
Fax: +679 337 0021

SPC Pohnpei Regional Office
PO Box Q,
Kolonias, Pohnpei, 96941 FM,
Federated States of Micronesia
Telephone: +691 3207 523
Fax: +691 3202 725

SPC Solomon Islands
Country Office
PO Box 1468
Honiara, Solomon Islands
Telephone: + 677 25543 /
+677 25574
Fax: +677 25547

Email: spc@spc.int
Website: www.spc.int